A Wideband Monopole Antenna Design

by
Jako Lourens

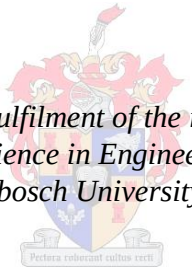

Thesis presented in partial fulfilment of the requirements for the degree
Master of Science in Engineering
at Stellenbosch University

Supervisor: Prof. KD Palmer
Department of Electrical & Electronic Engineering

March 2013

Declaration

By submitting this thesis I declare that the entirety of the work contained therein is my own, original work, that I am the sole author thereof (save to the extent explicitly otherwise stated), that reproduction and publication thereof by Stellenbosch University will not infringe any third party rights and that I have not previously in its entirety or in part submitted it for obtaining any qualification.

Date: March 2013

Acknowledgements

I would like to thank Electromagnetic Software and Systems (EMSS) for donating FEKO and allowing it to be used on this antenna design. Without it's use, complex mathematics would have to be performed manually – a nigh impossible task.

Abstract

The successful operation of a man-pack VHF jamming system requires a compact and efficient antenna operating over a wide bandwidth. The design of such an antenna is the focus of this thesis.

The antenna should be of a practical size for a portable system and it must radiate energy efficiently across a frequency bandwidth in excess of a decade. A practical 'target' specification of such an antenna has been drawn up based on the performance of a commercially available system.

Several possible antenna topologies, each with a variety of loading section options, are tested using "Full wave" electromagnetic modelling (FEKO). Each topology/loading-section is numerically optimised for load element values by considering both its gain and reflection coefficient. Results of the 'optimally loaded' solution for each topology are then compared to each other to arrive at the best overall design.

The best result is found to be the traditional monopole whip-type antenna, with four R-L loading sections spread along its length. The simulated results show that the proposed antenna can be expected to meet the target standing wave ratio (SWR) specifications while offering a gain advantage of between 5 and 10 dBi higher than is available commercially. The selected design is constructed and its performance measured.

Opsomming

Die suksesvolle werking van 'n mobiele VHF 'jammer' benodig 'n kompakte antenna met 'n bruikbare benuttingsgraad wat oor 'n wyeband funksioneer. Die ontwerp van so 'n antenna is die fokus van hierdie tesis.

Die antenna moet kompak genoeg wees om draagbaar te wees en moet 'n bruikbare benuttingsgraad hê oo r 'n frekwensie-bandwydte van meer as 10:1. 'n Praktiese spesifikasie is opgestel vir die antenna deur te kyk na die sigblaaie van beskikbare stelsels. "Volgolf" elektromagnetiese modelleringsagteware is daarna gebruik om 'n parametriese ondersoek te loods van verskillende antennas.

Verskillende topologieë is getoets met 'n verskeidenheid van belaaide seksies waar die topologieë ge-optimaliseer was vir wins en weerkaatskoëffisiënt. Die resultate vir elke optimale oplossing is vergelyk.Opgrond van hierdie resultate is bevind dat die beste topologie die tradisionele monopoolmas 'whip-type' antenna is met vier RL lading afdelings langs die lengte versprei. Analise word gebruik om te wys dat verwag kan word dat dit aan die aanwins en staande golf verhouding (SGV) spesifikasies sal voldoen met n 10 dB verhoging in aanwins vir n laer SGV.

Die geselekteerde ontwerp is gebou en gemeet om te verifieer dat dit aan die spesifikasies voldoen.

Table of Contents

List of Figures

Chapter 1

Introduction

1.1 Background

In today's digital age, protecting soldiers from their enemy involves having better weapons, more accurate information and better electronic shielding. Of growing concern are radio-controlled improvised explosive devices (RCIEDs) which are used in traps in urban environments where such devices are triggered by a radio signal to attain the highest impact. The best protection against such RCIEDs is to avoid detonation by jamming the enemy's RCIEDs communications link to allow the device to be safely defused or removal.

Figure 1: GMJ9000V Portable Jammer with reference antenna [8]

A typical wideband man-pack currently used to deactivate RCIEDs is displayed in figure 1. The jammer is mounted on a soldier's back in a metal case, 270 X 230 X 90 mm. From the case a 1.5m long whip antenna spans upward. This antenna is both flexible and foldable, allowing movement through doorways or under other obstacles.

Since the jammer is mounted on a soldier's back, it shouldn't interfere with the soldier's performance. The weight should also be kept to a minimum and should be easy to manipulate if needed. To ensure all round coverage he antenna must have an omni-directional azimuthal pattern with no pattern breakup. This transmitter is rated for 20 Watt continuous duty power handling and has a bandwidth stretching from 20MHz to 500MHz. The transmitter requires an antenna with a voltage standing wave ratio (VSWR) below 3:1, but typically 2.5:1, throughout the specified frequency band. Figure 3 shows the VSWR performance of an available antenna designed to have an input impedance of 50 Ohm.

When this 0.9kg antenna is folded to improve mobility it has a height of 0.85m. The antenna's gain variation over its frequency bandwidth has the lowest gain of -15 dBi at 20MHz which rises to a maximum of -4 dBi at 300MHz (refer to Figure 2).

This thesis discusses the design of an antenna with improved performance above that of this current antenna which is taken as the performance reference.

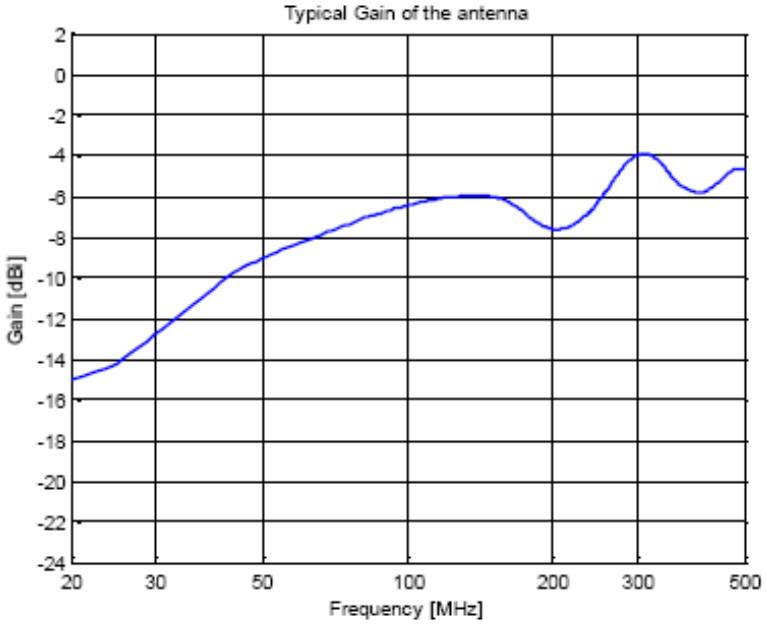

Figure 2: Measured OMNI-A0124-01 Antenna Gain from literature [8]

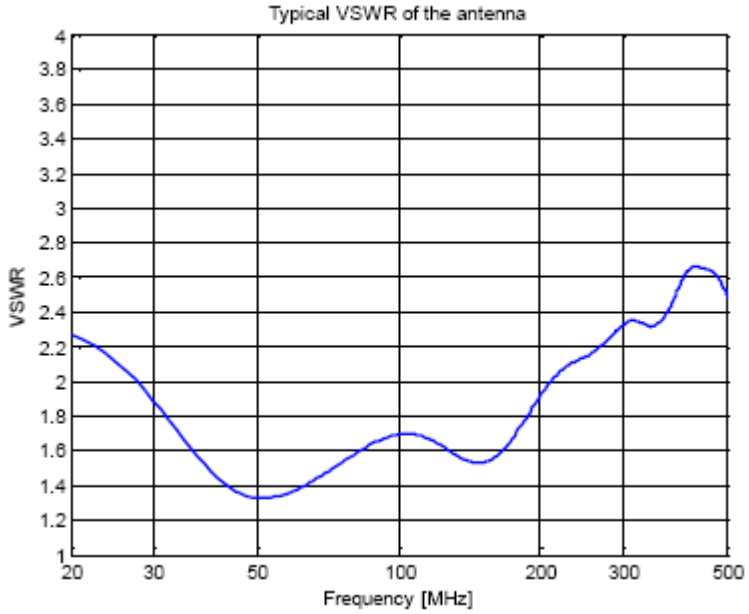

Figure 3: Measured OMNI-A0124-01 Antenna VSWR from literature [8]

1.2 Thesis outline

The omni-a0124 antenna in figure 1 is taken as the reference antenna design. As this is an electrically short antenna, no spatial gain increase can be achieved. So, if the power radiated is to be increased through “effective” gain increase the focus must be on increasing the antenna’s efficiency. As the power reflected obviously depends on the VSWR, the two electrical parameters of importance in the design are the Gain (or more accurately the efficiency) and the VSWR.

The antenna design specification, targets based on the reference antenna design, can be summarised as follows:

- Bandwidth from 20 MHz to 500 MHz
- The lower frequency gain should be higher than -14dBi and at the higher frequency gain should exceed -4dBi.
- The voltage standing wave ratio should be less than 3:1.
- It must be foldable to a length equal to or less than 0.85 m
- The unfolded whip should not exceed a length of 1.6 m and a diameter of 25 mm
- The feed power handling should allow for 30 W
- It must weigh less than 1 kg

Chapter 2

Literature study

As stated in Paragraph 1.2, for an electrically short antenna no significant spatial gain increase can be achieved by changing its shape. One standard way to improve bandwidth performance of such an antenna is by loading the antenna with various combinations of R, L and C circuits. Some aspects of 'loading' will be introduced as part of a literature discussion.

2.1 Monopole antenna loaded with non-Foster circuit

Zhang, Sun, Li, Wang and Xue [1] worked on the design of an antenna with a stable impedance and radiation pattern over a wide frequency range. Methods to reduce the dimensions of antennas were also investigated and a monopole antenna with a length less than λ/4 was introduced in their paper. The antenna becomes capacitive at low frequencies; it requires the use of a compensatory inductor to obtain real input impedance. The term adopted where the impedance has only a small imaginary part is "**resonance**".

The poor impedance matching of the antenna's input impedance due to the small radiation resistance at the lower frequencies will also hinder the antenna's abilities to radiate energy due to the high reflection coefficient. By adding inductive series elements and changing the position and values of the lumped elements the antennas current distribution and effective radiation pattern amplitude is changed, allowing wideband behaviour to be obtained.

The monopole antenna's bandwidth was extended and the dimension was reduced when it was loaded with several lumped elements composed of resistors, inductors and capacitors in different positions along a radiator. The antenna's efficiency was however low over the whole frequency range as its Q factor could not break through the Chu-Harrington limit where the Q value of a small antenna is relatively equal to the volume of a sphere that encloses it, thus the antennas bandwidth will shrink.

They used a technique presented by Sussman-Fort and Rudish regarding non-Foster impedance matching. Networks of negative inductors and capacitors were used to produce a non-Foster matching network where the network was used to bypass the restrictions of gain-bandwidth theory.

The concept adopted here is the addition of a variable inductor (non-Foster circuit) to try extending the "resonant" behaviour. The non-Foster circuit when compared to passive matching achieved higher efficiency over a wider bandwidth. The antenna's current distribution and radiation pattern stays unaffected by the use of a non-Foster circuit.

They present a monopole antenna with a length less than $\lambda/4$. Due to its length, the monopole antenna is mostly capacitive; this can be compensated for with the use of an inductor. The antenna can "resonate" at different frequencies if the value of the inductor is changed. It is considered, from these results, that a monopole antenna should be loaded with a non-Foster circuit to obtain resonance over a broad frequency range.

The bandwidth could be increased if the inductor's inductance could be changed to the reactive values needed to obtain the required impedance properties as given in Paragraph 1.2, over a wide frequency range. Jjj you should automate your fig numbers – it is an easy skill worth knowing

Zhang et al proposed a non-Foster circuit constructed from inductors and capacitors with positive and negative element values, used as illustrated in Figure 4. This circuit will act as an element with a negative reactance slope, which will allow resonance at the frequency depending what reactance is required (refer to Figure 5). Thus if the wire, with a length smaller than $\lambda/4$, impedance is transformed to the required reactance, shown on figure 5, the wire will resonate at that depended frequency. The admittance of a network will increase when Foster elements, L and C, are applied to the network.

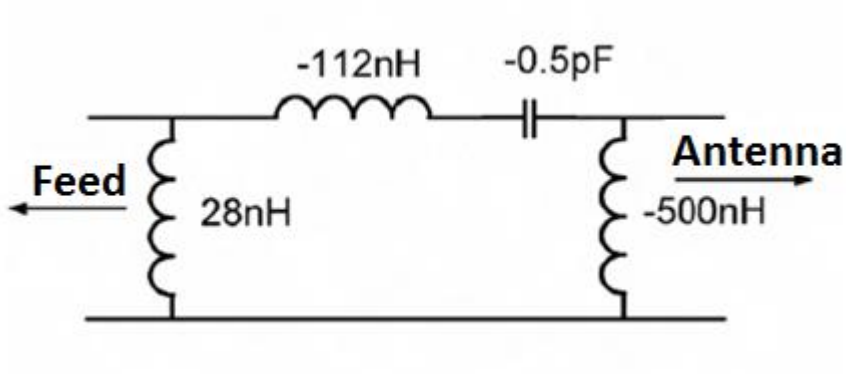

Figure 4: non-Foster circuit schematic

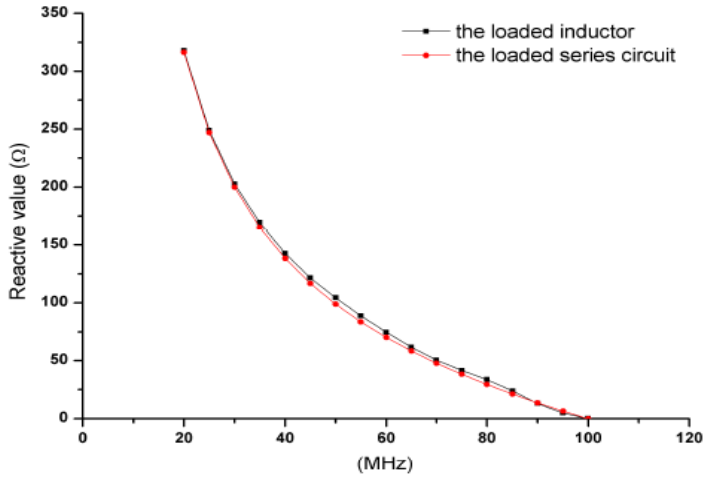

Figure 5: Reactive value required for an antenna length of $\lambda/4$ to achieve resonance at a frequency [1]

The input reactance and resistance with and without the addition of a non-Foster circuit are illustrated in Figures 6 and 7. As shown in these figures, without the Foster circuit the antenna's impedance, especially at the low frequencies, is capacitive and the radiation resistance is so small that the energy concentrating near the antenna could not be radiated.

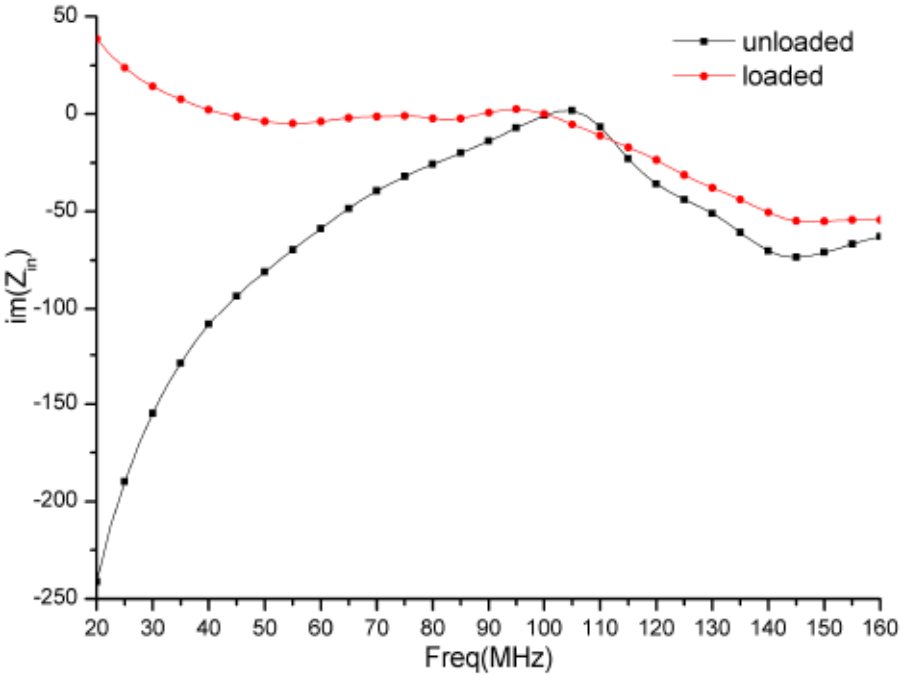

Figure 6: The value of the input reactance with and without non-Foster circuit loading [1]

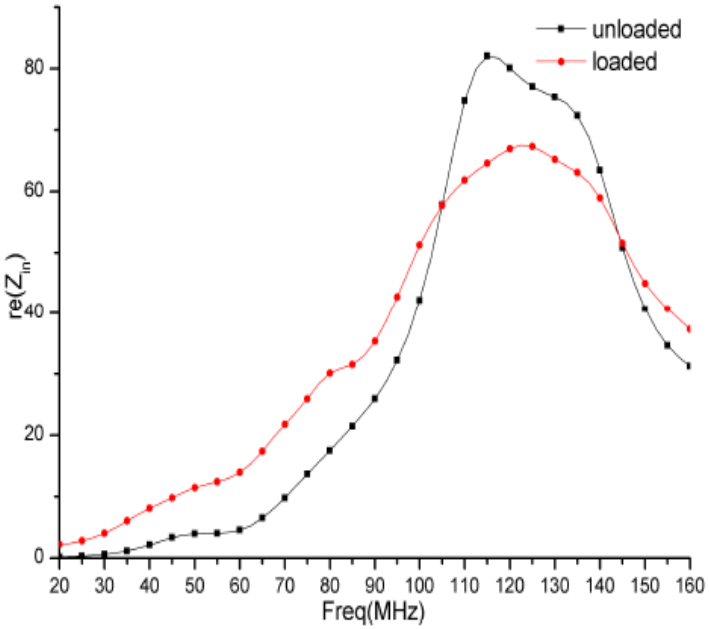

Figure 7: The value of the input resistance with and without non-Foster circuit loading [1]

With the non-Foster circuit loaded, the reactance of the antenna is smaller than the unloaded antenna over the wide frequency range with slight variances over frequency making the non-Foster loaded monopole antenna better matched over the frequency range..

The unloaded monopole antenna bandwidth with VSWR < 3 is between 85 MHz and 130 MHz, where the bandwidth of the loaded antenna is between 65 MHz and 150 MHz, the non-Foster circuit has increased the bandwidth by 90%. An optimization algorithm based software designed to calculate matching networks was used to obtain a passive matching network to further increase the bandwidth, which is also illustrated in Figure 8.

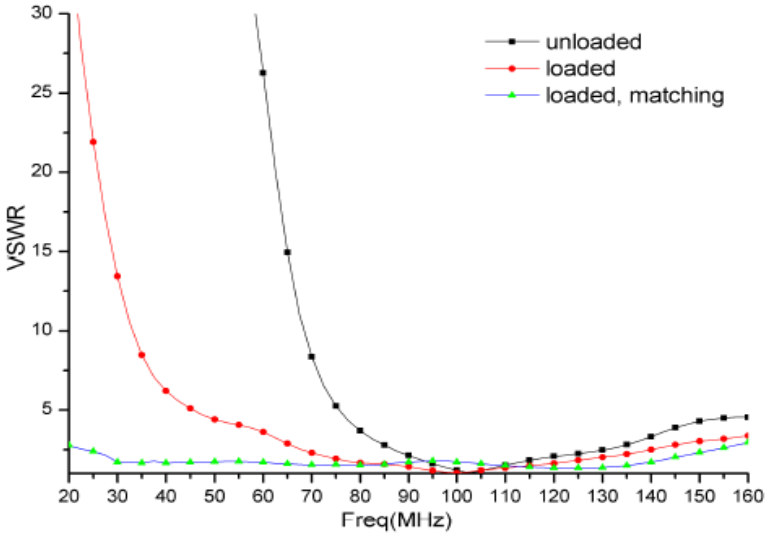

Figure 8: The values of the VSWR with and without non-Foster circuit loading [1]

The radiation patterns of the loaded and unloaded monopole antenna are depicted in Figure 9. The radiation pattern of the loaded antenna is more stable over its bandwidth, where the unloaded monopole antenna's pattern deteriorates. The bandwidth obtained using this technique is too narrow to meet the specifications.

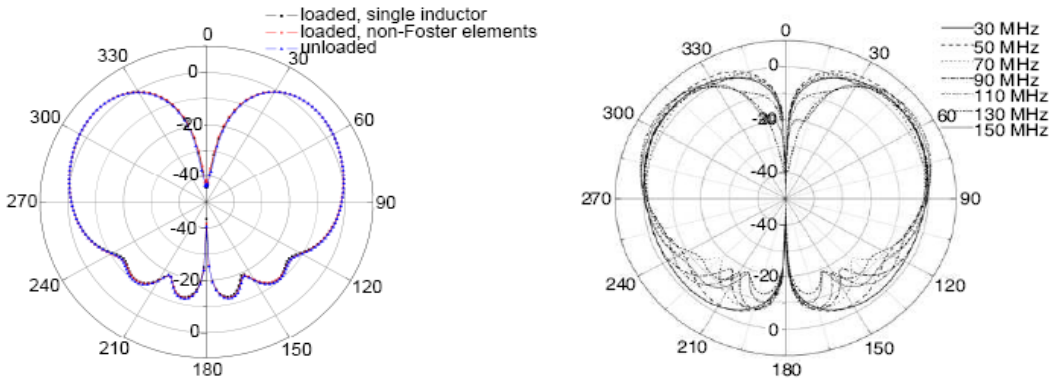

Figure 9: Radiation pattern of loaded (left) and unloaded (right) monopole antennas. [1]

2.2 The Short Loaded Monopole analysed by Hansen, Stewart and Harrison

Hansen [2], in a paper that relates to the current discussion on short loaded monopole antennas, mentions the following with regard to the principle of antenna loading:

"In principle the loading inductor functions by keeping the current distribution nearly (emphasis added) constant from the feed to the load point, thereby increasing the current moment. Since the transmitting parameter, radiation resistance, varies as current moment squared, and since the receiving parameter, effective length, varies with the current moment, it is clear that inductive loading will improve short monopole performance. There is a value of loading reactance which allows the current to approximate a constant value out to g·h (the fractional distance of the coil position from the feed) with a linear drop-off beyond. This value of inductance is, however, insufficient to produce input impedance resonance. The resonant value of load produces a modest current peak (emphasis added) just beyond g·h so that the current moment is increased by an additional amount over that expected from the constant current model."

Stewart [3] pointed out that Devoldere's paper [10] about Low-Band DXing (receiving and identifying distant radio or television signals) and Brown's paper [11] on mobile antennas, fail to show the current peak in shorter (< 0.1 lambda) loaded antennas. He tried duplicating the Hansen and Cebik [2] findings that the current distribution along a radiator has a direct impact on the efficiency, but that didn't appear to be the case. Referring to Hansen: *"radiation resistance varies as current moment squared".* The change in the radiation resistance impacts the efficiency, thus the gain of the radiator. According to Stewart, an unloaded, no-resonating monopole has the same efficiency as a resonating monopole of the same size. The current distribution will only have an effect on the radiation resistance when loss is introduced.

Harrison [4] analysed the loaded monopole using superposition of asymmetrically excited dipoles. He calculated the input impedance, current and loading inductor currents for several lengths, with various loading coil Q values.

There seems to be a gradual increase in efficiency as the load point moves closer to the ends of the antenna. His data stopped with the loading point's position 2/3 from the antenna's feed. Method of Moments (MoM) calculations were made by Hansen over several years and indicated that the maximum efficiency point for the loading occurs closer to the feed.

The current should rise from the feed to a modest peak near the load point and then decay. This will improve radiation resistance over an unloaded monopole. A point can then be chosen to give input impedance closer to 50 Ω with some loss in efficiency.

In conclusion, the previous authors' theories were combined to design an improved antenna. Zhang et al showed that a change in input reactance would be needed to

resonate over a wide frequency range. This will make the impedance stable for matching. Hansen stated that the current should rise from the feed to the first RL loading point and decay for the best efficiency. Stewart added that the current distribution will only have an effect when loss is introduced. Loading points towards the end of the antenna were investigated with MoM calculations, as indicated by Harrison and pointed out in his paper.

2.3 Frequency enhanced monopole design

Richard E Deasy and Cedar Rapids [7] designed an antenna with a length substantially less than one quarter wavelength at the operational frequency. A large number of inductors, installed in series with the wire, were used to enhance the antenna's bandwidth. These inductors were isolated from one another so as to have negligible mutual inductive coupling. The inductors' size must be kept to a minimum to avoid individual resonance within the operating frequency range. Inductors with progressively greater inductance values are spaced closely together towards the end of the antenna.

They believed the best performance might be achieved when the distance between the inductors decreased logarithmically as the inductance increased towards the end of the antenna. Any positioning pattern with an increasing inductive loading in a linear fashion towards the end will be beneficial.

2.4 Effect of Ground-Plane on antenna performance

As the antenna to be designed is operated close to the earth's surface, the issue of whether the earth should be considered as a ground plane was addressed. Antenna characteristics are generally derived by assuming the antenna to be in free-space. A monopole antenna can be realised and analysed as a dipole when an infinite, perfect conducting ground plane is introduced. This is known as the method of images, were the ground plane is removed and an image antenna is supplemented to mimic the signal reflection associated with the ground plane. An antenna's most important characteristics, antenna pattern and terminal impedance, will be altered with the addition of a ground plane in the vicinity of the antenna.

An antenna, will in general, radiate without a ground plane, but with a pattern and impedance different to those of an antenna above a ground plane. A ground plane can be seen as a reflector of energy from the antenna itself, which sets up constructive and destructive interference of signals in space which, in turn, alters the antenna pattern. The parasitic capacitance from antenna to ground plane alters the antenna's terminal impedance.

Tom Yestrebsky's [5] paper that relates to the design of a wireless system and the effect a ground plane has on an antenna system, mentions the following:

For applications where one has the luxury to use or not use a ground plane, the choice is not particularly clear. If, by using a ground plane, the modified antenna pattern, directionality, and terminal impedance yield the best system performance, then it should be used. Otherwise it is not advisable. For applications where a ground plane must exist, or where no good ground plane can be allowed, the antenna should be optimized for that particular condition. Finally, there is no reason an adequate antenna cannot be constructed, even if there is no good ground plane to work against.

In determining a design for this wideband monopole antenna the advice of Tom Yestrebsky is followed - all electromagnetic modelling will assume the addition of a perfect electrically conducted ground plane.

2.5 Realised Gain:

The term *realised* or *apparent* gain is used in this work when the mismatch loss is added to the strict definition of gain. The apparent gain is an important parameter in this work as it includes the effect of the antenna's standing wave ratio (SWR) and efficiency in one parameter. This may then be taken as the *figure-of-merit.* Apparent/realized gain can be defined as:

Realized_gain = Directivity X Radiation_efficiency [Def1]

Realised_gain =|s21|²X directivity

The forward transmission coefficient (S21) can be calculated using the antenna's reflection coefficient (S11) with the following equation

$$|S21|^2 = (\,1 - |S11|^2\,)\textit{[1]}$$

This will determine the gain of the antenna with the power decrease due to reflected power taken into account.
The radiated power, P_r *, of the antenna would therefore be:*

$$P_r = P_i.(\,1 - |S11|^2\,).\eta \qquad [2]$$

η - radiated efficiency

P_i *- incident power*

Clearly, realised gain is always <=true gain.

2.6 Conclusion from Literature

After examining the above mentioned papers we can conclude the following:

- The current distribution on the antenna may be changed from the triangular unloaded case to yield an improved gain and radiation power.

- The antenna's impedance must be managed so as to meet the standing wave ratio requirement.

- The antenna's current distribution and impedance can both be changed through the use of inductive and resistive loads located at different positions on the antenna.

Zhang et al advised that to achieve an improvement in the antenna's impedance and efficiency; the load's impedance should change with a certain gradient by using negative inductors and capacitors.

To achieve the goals set out in Paragraph 1.2, the work of Richard E Deasy, Cedar Rapids and Robert Hansen will be used by positioning inductors on an antenna to reduce its capacitance and alter the antenna's current distribution.

Chapter 3

Simulations and Analysis of Antenna Designs

This paragraph presents a brief synopsis of the antenna development and results.

The design process normally starts by considering what building blocks are available to meet the requirements, and in this case an inductor is obviously the element of choice with a high inductance being needed over a wide bandwidth. As available commercial inductor's inductance value decreases with an increase in frequency and bandwidth, it will be shown that the best results are obtained when using a number of series inductors for realisation.

The required inductance can be realised in two ways, ferrite beads or chip inductors. The term ferrite "**bead**" is used to denote a toroidal type ferrite core which is slid over the metallic rod/whip of the antenna, while "**chip**" refers to a conventional inductor inserted in series between rod/whip sections. The bead is considered first.

The ferrite bead is placed over the antenna with, the antenna passing through the bead. Refer to Figure 12 in Paragraph 3.1. Although it is at first counter-intuitive to see this bead as adding a series inductor, an imaginary wire can be considered as closing over the bead to form the single turn. The available ferrite material found to use for this design was Perminvar with a working frequency range between 10MHz and 200MHz with one turn around this ferrite bead providing an inductance of 330nH. Practically the imaginary wire is replaced with a resistor to add resistivity in parallel to the inductance so as to reduce the reflected current's amplitude.

The second inductance realisation option investigated is the use of "chip" inductors with the RL chip sections using one or a number of series inductors connected over a parallel resistor. Refer to Figure 11 in Paragraph 3.1 for a diagram of the RL chip section.

With two inductance realisation options available the first topology investigated was that of the monopole antenna loaded with the RL bead sections, refer to Figure 10(a). The inductance that the bead could provide was fixed at 330nH as it can only have one turn. The number of RL bead sections loaded on the antenna was varied to change the inductance added and the use of four, five, seven and even nine RL bead sections did not provide significant gain and impedance improvement.

After establishing that bead sections do not offer sufficient inductance to improve the monopole antenna's performance, a topology change was investigated. The topology used first is popular in low frequency communications: The top-loaded antenna (refer to Figure 10(b)). This antenna is again loaded with various RL bead sections positioned at various positions during the optimisation process to determine the optimal resistance and position. The number of RL bead sections used in the simulation was four, five and seven and as with the monopole even using seven bead sections it is again shown that the low bead inductance cannot significantly improve the antenna's performance, making it clear that higher inductance RL chip sections should be used.

The next topology focussed on increasing the antenna's length using RL chip sections at four locations on the antenna at fixed locations as the position did not make a significant difference in previous simulations. The antennas length was increased by "winding" it into a helix structure that would allow a longer wire within the 1.6 m height restriction (refer to Figure 10(c). The inductance required was investigated using three inductance values starting at 1 µH. This was increased to an inductor of 2 µH which could be obtained with two of the previous inductor in series etc. Finally the optimisation yielded an inductance of 18 µH that cannot be obtained for this bandwidth.

After exhausting the loaded helix structure a different topology was attempted to again increase the antenna's wire length. By simply folding the antennas at the top by 180° the length can be increased by 800mm (refer to Figure 10(d) because the antenna should be able to fold halfway to avoid obstructions. This folded antenna is loaded with RL chip sections between 1 µH and 18 µH.

All the above simulations were optimised with the required goals being

1. a reflection coefficient less than 0.5 to give a VSWR less than 3 and
2. a gain higher than -10 dB across the bandwidth.

As none of the above yielded a satisfactory result the last topology chosen was again the simple monopole antenna, but loaded with RL chip sections (refer to Figure 10(e)).
Optimisations were performed on the antenna loaded with four RL chip sections with similar inductance values of 1 µH, 2 µH and 18 µH used and with resistor values ranging between 0 Ω and 1 kΩ.

The optimisation showed that an inductive load of 2 µH could potentially improve the antenna's impedance and the performance to meet the specifications across the required bandwidth.

The next step was to find suitable commercial inductors. Datasheets showed that the only way to realise a 2 µH inductor for the frequency range was to make use of inductors in series. The inductor selected is provided by Coilcraft which has a 560 nH inductor capable of operating between 1 MHz and 900 MHz. The supplied inductor's measured S-parameters were imported into FEKO in order to model the actual non-ideal inductance and resistance. It was found that the number practical inductors used in the RL chip section needed to be increased to six (theoretically 6*0.56=3.4 µH) to have a similar performance as the 2 µH ideal case.

The final antenna design was compared to the reference antenna's VSWR and gain to determine the improvement in performance. The new antenna design had a similar VSWR to that of the reference antenna, keeping below 2.5 where the reference antenna reaches 2.7 at the high frequency. When comparing the gain of the final antenna and the reference antenna to each other a satisfactory improvement can be observed in the antennas performance having a gain of 5 to 10 dB higher across the bandwidth.

The following sections will describe the results mentioned above in detail.

Table 1 provides an overview of the results. Each of the rows represents a topology/loading-section combination with the values of the loads having been optimised. Entries in the row show, as a percentage, over how much of the frequency band the antenna meets the specifications at the top of VSWR, gain and efficiency, with the last column showing when both gain and VSWR are met simultaneously. The cells of the table are coloured with green-yellow--orange-red as 100% to 0% to allow visual selection.

A good design should thus

- meet the VSWR over the whole band (first column 100% green), and
- have as much gain as possible (second and last column as far away from red as possible).

Taking the first row as an example: This antenna has satisfactory S11 over only 17% off the band; and high gain over 84%; and high efficiency over the whole band. However the last and most important column shows that this antenna works well only over 2% of the band.

Simulation 22 is the final antenna design using ideal inductors of 2 μH.

The results for the monopole using six practical series 1008HT-R56T inductors with imported S-parameters are simulation 24

	Percentage specification was met over bandwidth [%]				
Simulation	VSWR < 3	Gain > -4	Efficiency	VSWR & GAIN	Description
1	17	84	100	2	Monopole with four RL Bead sections at fixed locations
2	17	84	100	2	Monopole with five RL Bead sections at fixed locations
3	17	84	100	2	Monopole with seven RL Bead sections at fixed locations
4	12	89	100	2	Monopole with nine RL Bead sections at fixed locations
5	17	84	100	2	Monopole with five RL Bead sections at various locations
6	19	77	100	8	Top-loaded antenna with four RL Bead sections at various locations
7	19	77	100	8	Top-loaded antenna with five RL Bead sections at various locations
8	79	30	21	16	Top-loaded antenna with seven RL Bead sections at various locations
9	74	76	34	21	Top-loaded antenna with four RL Chip sections at various locations
10	69	51	22	8	Top-loaded antenna with five RL Chip sections at various locations
11	82	11	19	0	Top-loaded antenna with seven RL Chip sections at various locations
12	83	9	7	0	Monopole with helix structure and short pitch length.
13	98	6	15	2	Monopole with helix structure, larger pitch length and four 1 uH RL chip section
14	41	24	27	11	Monopole with helix structure, larger pitch length and four 2 uH RL chip section
15	95	29	20	6	Monopole with helix structure, larger pitch length and four 18 uH RL chip section
16	100	17	17	5	Monopole with folded structure and four 1 uH RL chip section
17	100	18	18	5	Monopole with folded structure and four 2 uH RL chip section
18	98	41	25	28	Monopole with folded structure and four 18 uH RL chip section
19	98	7	12	2	Monopole antenna with four 1 uH RL chip section
20	91	7	13	0	Monopole antenna with four 2 uH RL chip section
21	91	13	19	5	Monopole antenna with four 18 uH RL chip section
22	100	55	33	31	Monopole antenna with four 2 uH RL chip section
23	100	68	40	44	Monopole antenna with four 4x1008HT-R56T loads at fixed locations
24	100	63	40	57	Monopole antenna with four 6x1008HT-R56T loads at fixed locations
25	66	65	34	44	Monopole antenna with four 6x1008HT-R56T loads at fixed locations with human body

Table 1: Percentage simulation met the VSWR and Gain specification

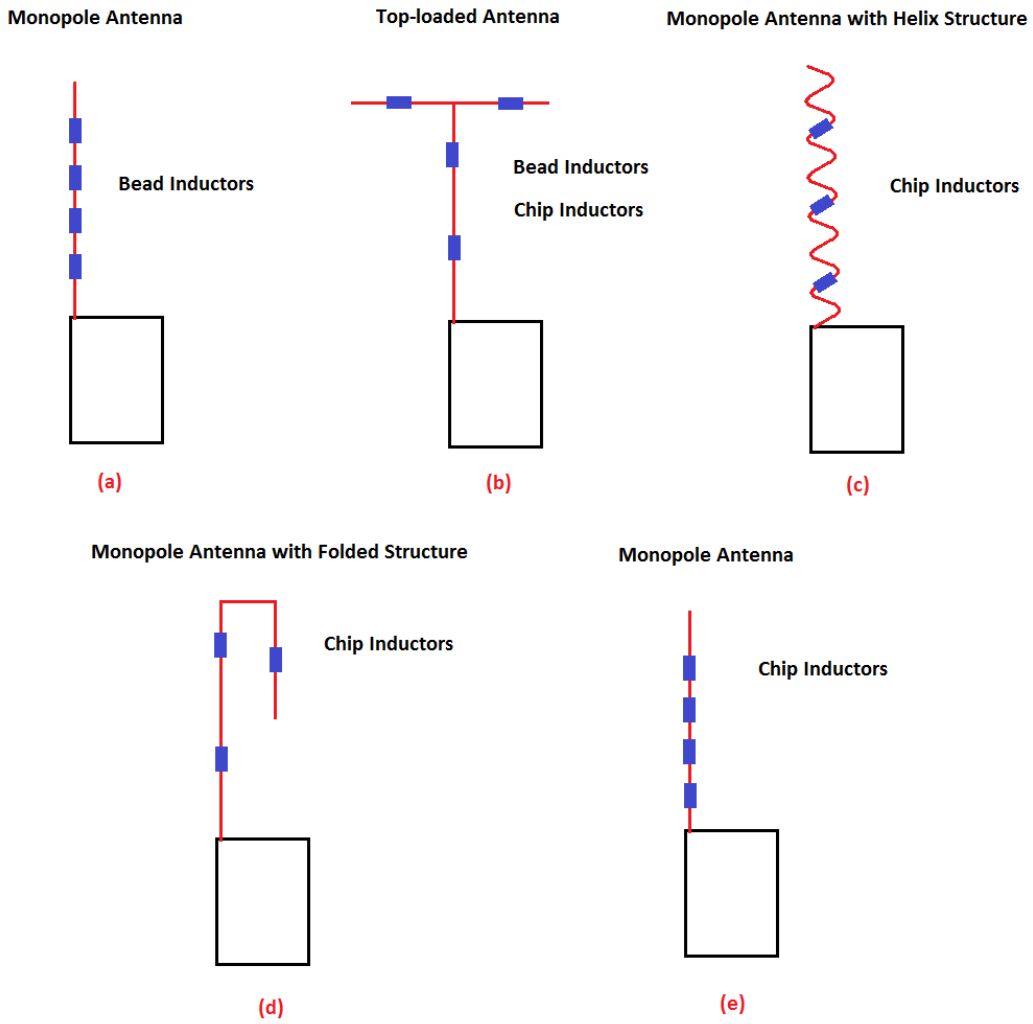

Figure 10: Design topologies investigated

Overview of simulations performed:

Optimisation for the best reflection coefficient and gain was performed on the following antenna designs. Antenna designs containing RL bead sections are discussed in Paragraph 3.2. The use of a load containing a higher inductance is investigated on various topologies in Paragraph 3.3. The final antenna design is discussed in Paragraph 3.4.

Paragraph 3.2

- Monopole with four resonant RL bead sections at fixed locations failed to meet specification.
- Monopole with five resonant RL bead sections at fixed locations failed to meet specification.
- Monopole with seven resonant RL bead sections at fixed locations failed to meet specification.
- Monopole with nine resonant RL bead sections at fixed locations failed to meet specification.
- Monopole with five resonant RL bead sections at varying locations failed to meet specification.

- Top-loaded antenna with four resonant RL bead sections at varying locations failed to meet specification.
- Top-loaded antenna with five resonant RL bead sections at varying locations failed to meet specification.
- Top-loaded antenna with seven resonant RL bead sections at varying locations failed to meet specification.

Paragraph 3.3

- Top-loaded antenna with four RL chip sections at varying locations failed to meet specification.
- Top-loaded antenna with five RL chip sections at varying locations failed to meet specification.
- Top-loaded antenna with seven RL chip sections at varying locations failed to meet specification.
- RL chip loaded monopole with helix structure failed to meet specification.
- RL chip loaded monopole with folded structure failed to meet specifications.
- RL chip loaded straight monopole with 2 μH inductors met the required specifications.

Paragraph 3.4

- Including the 1008HT-R56TInductor S-parameter model into the FEKO loaded monopole simulation, simulations showed that six series inductors would be needed, giving an inductance of 3.36 μH.

3.1 Construction of Inductors

In this chapter a ‘bead’ section refers to an inductor formed by sliding a ferrite bead over the continuous monopole conductor (Figure 12), while a ‘chip’ inductor refers to a normal commercially available chip inductor which, of course, requires that the monopole be cut so that it can be inserted in series (Figure 11).

A parallel resistor will be attached to the bead and chip inductor, producing the diagram Figure 13, in order to change the antenna’s impedance. The bead and chip sections will induce resonance over the required operating frequency range.

The parallel bead inductor will have an inductance of 330 nH between the operating frequency (10 MHz to 200 MHz) of the ferrite material. Inductors with different operating frequencies are commercially available. The required size of inductance can be achieved by placing smaller inductors with the desired operating frequency in series with each other.

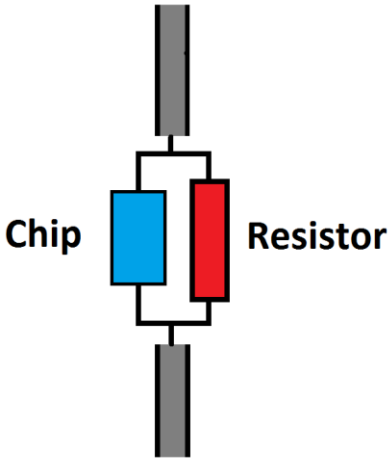

Figure 11: RL Chip section

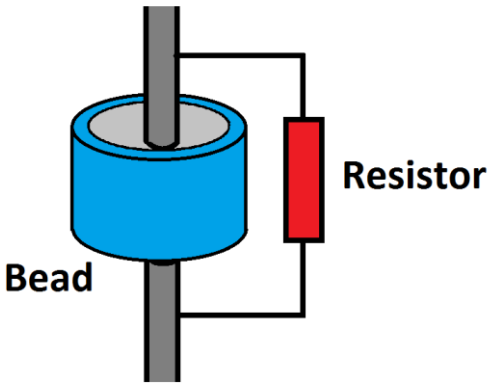

Figure 12: RL Bead section

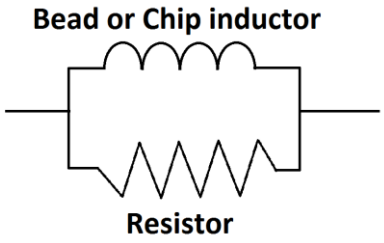

Figure 13: RL Bead and Chip Diagram

3.2 Topologies containing Bead inductors

3.2.1 Monopole antenna with RL beads at fixed and various locations

The first topology investigated to meet the required specification, was the monopole antenna loaded with RL bead sections. The monopole antenna was loaded separately with: four, five, seven and nine RL bead sections at fixed locations (refer to Figure 14). The monopole antenna was also loaded with five RL bead sections at various locations to investigate the effect of the beads location on the antenna's performance.

The RL beads of the first monopole antenna were spaced 300mm from one another starting 300mm from the feed. The RL beads of the second antenna model were located at the following distances from the feed:

200 mm, 500 mm, 800 mm, 1000 mm and 1400 mm. The RL beads for the third and fourth model were both spaced 200mm from each other starting 200mm from the feed. The last model of this section had RL bead sections at various positions.

The model was optimised with the goal of having a reflection coefficient lower than 0.5 while having a gain higher than -10 dB. The antenna with five RL beads at fixed and various

locations have equal gain and SWR therefore the position of RL beads will not have an effect on the antenna's characteristics as Figure 15 illustrates. Neither one of the simulations meets the specification of the SWR lower than three nor a gain higher than -14 dB across its bandwidth

This topology will not meet the specifications as required and therefore the top-loaded antenna with RL bead and chip sections must be investigated.

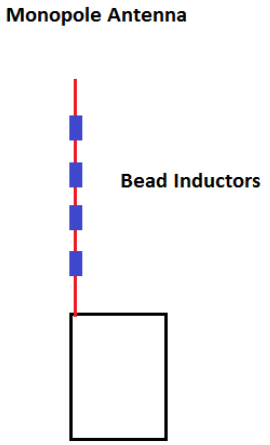

Figure 14: Monopole antenna with RL Bead sections

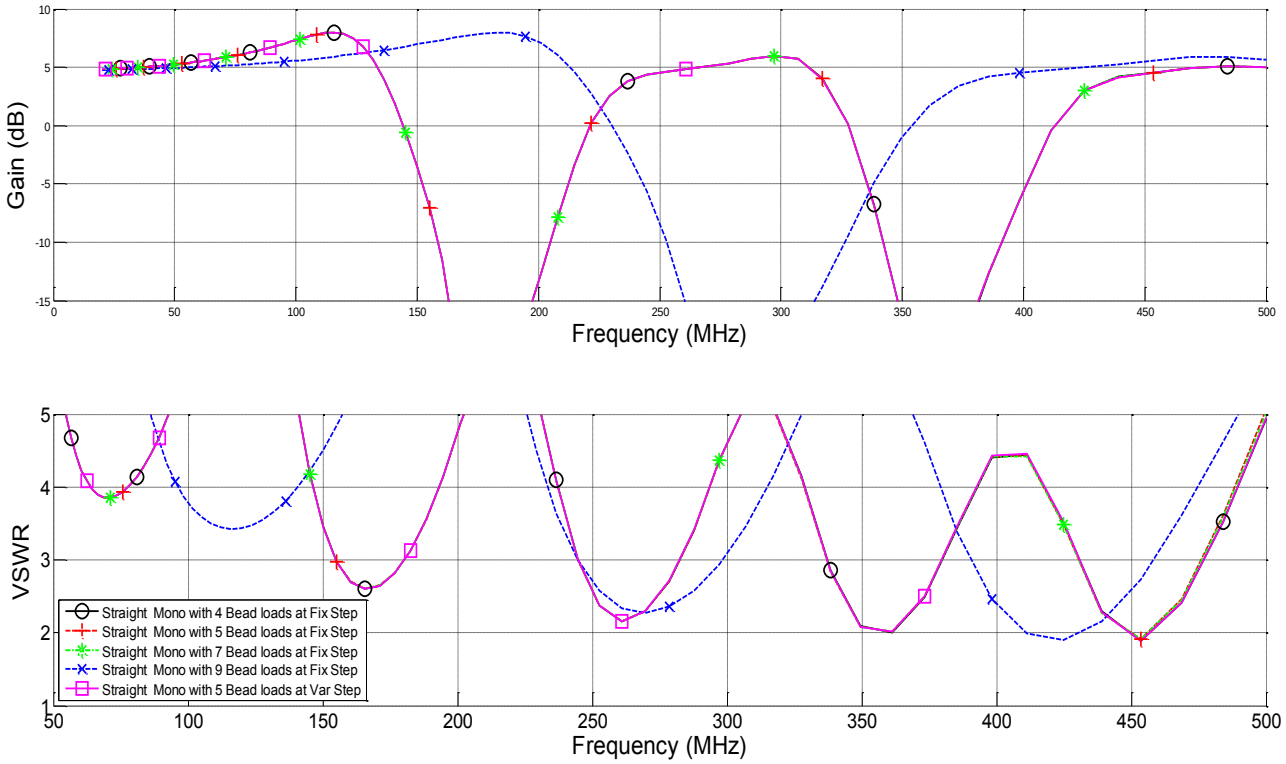

Figure 15: The gain and SWR of monopole antenna with four, five, seven and nine RL Beads at fixed locations (Fix Step) and various locations (Var Step)

3.2.2 Top-loaded antenna with RL bead and RL chip sections at various locations

The top-loaded antenna was considered because of its common use for low frequency communications. Antenna models were optimised with four, five and seven RL beads at various locations (Figure 16), by assigning an area to each inductor.

Boundaries were set for each bead from which a position was chosen during the optimisation process. The resistance value had n boundary between 0 Ω and 1 kΩ.

The following boundaries conditions were set for the antenna with four, five and seven RL beads:

- Antenna with four RL beads: 0mm, 800mm and 1600mm
- Antenna with five RL beads: 0mm, 400mm, 900mm and 1600mm
- Antenna with seven RL beads: 0mm, 400mm, 700mm, 1000mm, 1300mm and 1600mm

Two RL beads were located on the horizontal wire at the top of the antenna. RL bead was located in the middle of each horizontal arm extending between 50mm and 300mm. The antennas gain, SWR and efficiency graphs are plotted in figure 17. The antennas with four and five RL bead sections have a gain higher than -15 dB, with a VSWR higher than three across most of the bandwidth. The antennae containing the four and five bead sections have 100% efficiency across the bandwidth and aren't displayed on the graph. The beads contain a low inductance which short-circuits the parallel resistor allowing for a higher current and thus a high efficiency.

Only when seven RL Bead sections are used the VSWR decreases to lower than three across most of the bandwidth, excluding between 30MHz and 60 MHz. The addition of more loads on the antenna started to affect the antenna's efficiency, having a maximum efficiency of 50% at 500MHz.

It was clear the inductance must be increased to obtain a VSWR less than three across the bandwidth. The use of RL chip sections must be investigated.

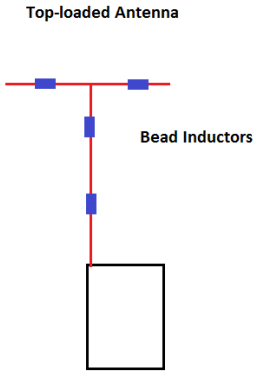

Figure 16: Top-loaded Antenna with RL Beads sections

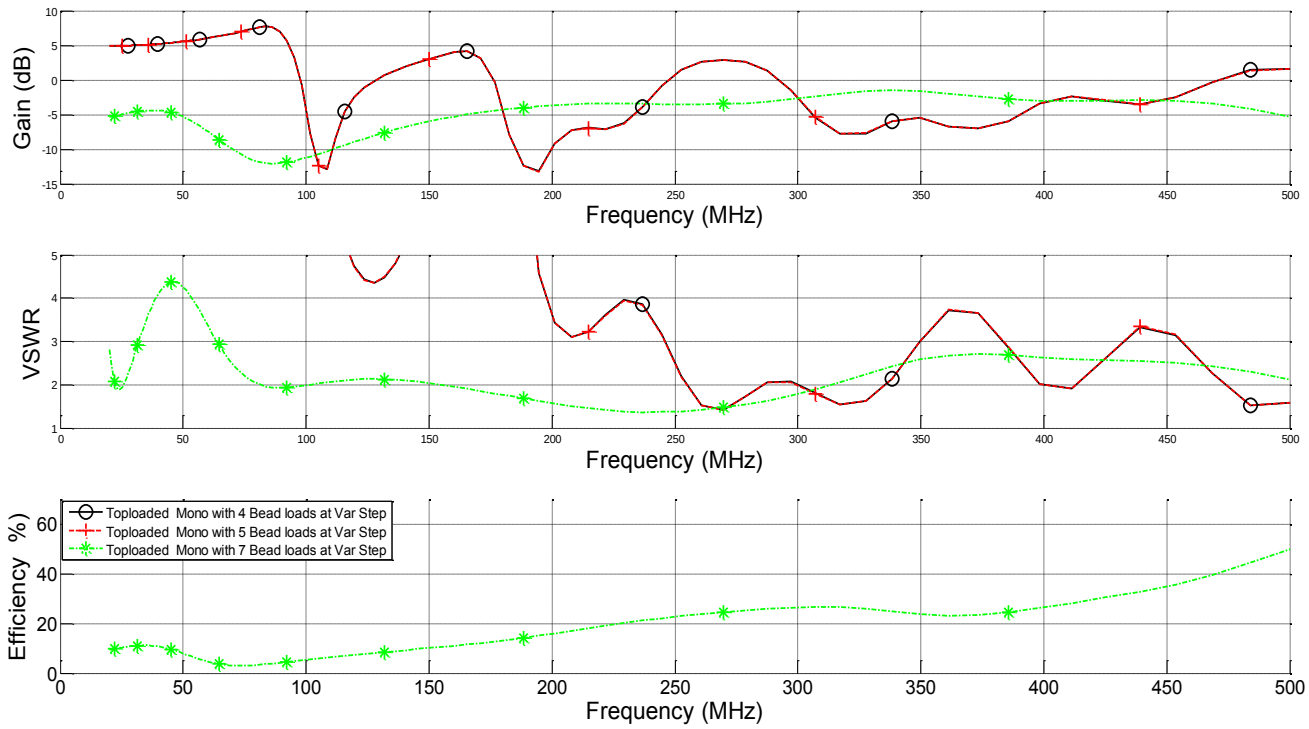

Figure 17: The gain and SWR of Top-loaded antenna with four, five and seven RL bead sections

3.3 Topologies containing chip inductors

3.3.1 Top-loaded antenna with RL chip sections at various locations

It was clear that more inductance was required to reduce the antennas SWR as the gain specification was met when RL beads were used but not the standing wave ratio. The inductance was increased using RL chip sections on the top-loaded antenna (Figure 18). RL chip sections consist out of a 1µH inductor and a parallel resistor between 0Ω and 1kΩ.

Similar boundaries were used on the RL chip loads than on the RL beads as presented below:

- Antenna with four RL chips: 0mm, 800mm and 1600mm
- Antenna with five RL chips: 0mm, 400mm, 900mm and 1600mm
- Antenna with seven RL chips: 0mm, 400mm, 700mm, 1000mm, 1300mm and 1600mm

Figure 19 indicates that the use of RL chip loads decrease the antenna's capacitance reducing the reflection coefficient decreasing the SWR. The addition of more RL chip loads to the antenna will reduce the SWR at 20MHz but will increase at higher frequencies as seen in Figure 19. All the RL chip loaded antennas will meet the gain specification for they are higher than -14dB across the bandwidth.

The top-loaded antenna will not be a usable solution because of fluctuations SWR across the bandwidth. By reducing SWR at 20MHz and 275MHz by adding more inductance increases SWR at 50MHz and 350MHz. Thus the antennas SWR won't be less than three across the bandwidth by increasing the inductance added.

The next topology investigate will be a monopole antenna with a helix structure loaded with RL chip sections.

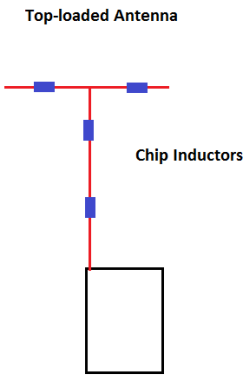

Figure 18: Top-loaded Antenna with RL Chip sections

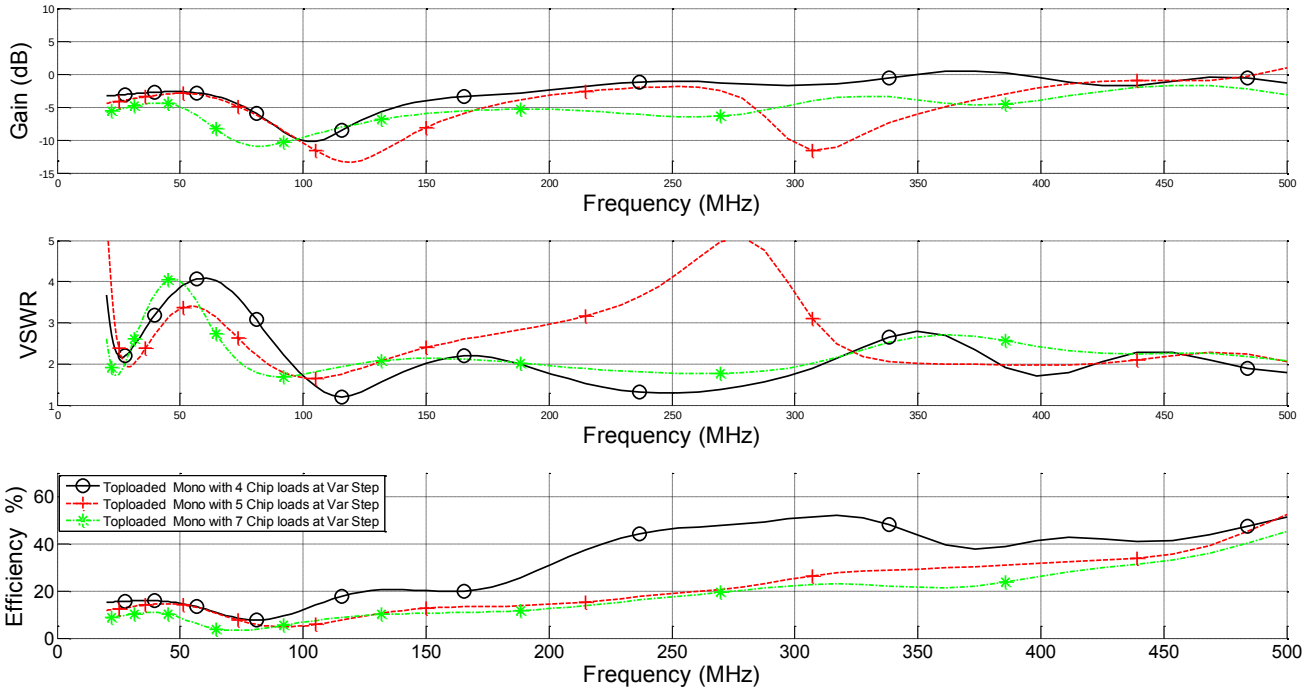

Figure 19: The gain and SWR of Top-loaded antenna with four, five and seven RL chip sections

3.3.2 Monopole antenna with a helix structure and RL chip sections at fixed locations

Another design option would be to curl the antenna into a helix, thereby increasing the length of the antenna but keeping to the maximum height of 1.6 meters (Figure 21). Capacitance will be added to the antenna's impedance if the distance from curve to curve in the helix structure becomes too short. The antenna's length will increase if a shorter distance from curve to curve (Dimension C in Figure 20) is used. This will allow more wire in the specified allowed height.

The number of loads used must be kept to a minimum to prevent effecting the antenna's SWR and gain at the high frequency. A simulation was performed where the pitch length was set to a minimum of 10mm to increase the total length of the wire.

Four RL chip loads, with an inductance of 1 µH, were spaced 300mm from each other starting 300mm from the feed. The antenna model with the small pitch length was optimised for a SWR less than 3 and gain higher than 10dB. The SWR is suitable at 20MHz but exceeds 3 at the higher frequencies as a result of the capacitance added to antenna's impedance by the closely positioned curves. This is the result of the small pitch length (Dimension C in Figure 20) used to increase the antenna's length.

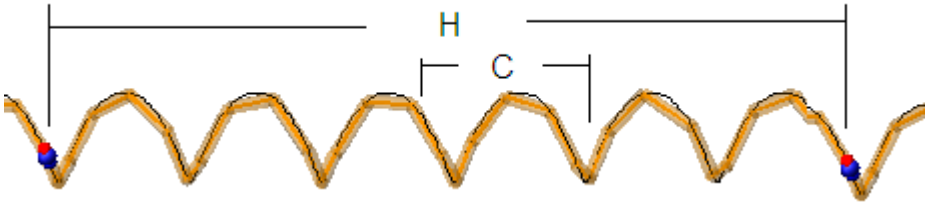

Figure 20: Helix antenna loading dimensions

It was required to use a large pitch length of 200mm to reduce the capacitance added to the antenna's impedance. Three inductance loads were used, 1 µH, 2 µH and 18 µH to investigate the inductance required to counteract the antenna's capacitance. The antenna with a 1 µH inductor meets the SWR specification over its bandwidth except at 20MHz but its gain drops far below -14dB at 350MHz.

The antenna does not meet the gain and SWR specifications when the inductance is increased to 2 µH. Then antenna's gain is increased and SWR is improved (except at 20MHz) when an inductance of 18 µH is used, refer to Figure 22.

The addition of more inductance will allow the antenna to meet the SWR specification but will not allow the antenna to meet the gain specification. This is made visible in Figure 22 when the magnitude of the antenna's gain experiences large drops at different frequencies.

The monopole antenna with helix structure will not be a valid solution for the required specifications. Another topology where the antenna's length can be increased must be investigated.

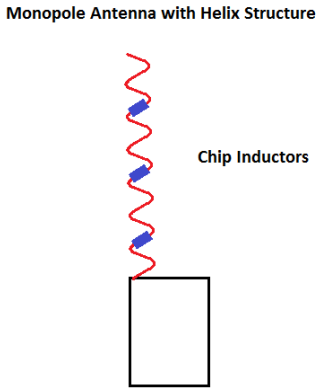

Figure 21: Helix monopole antenna with RL chip sections

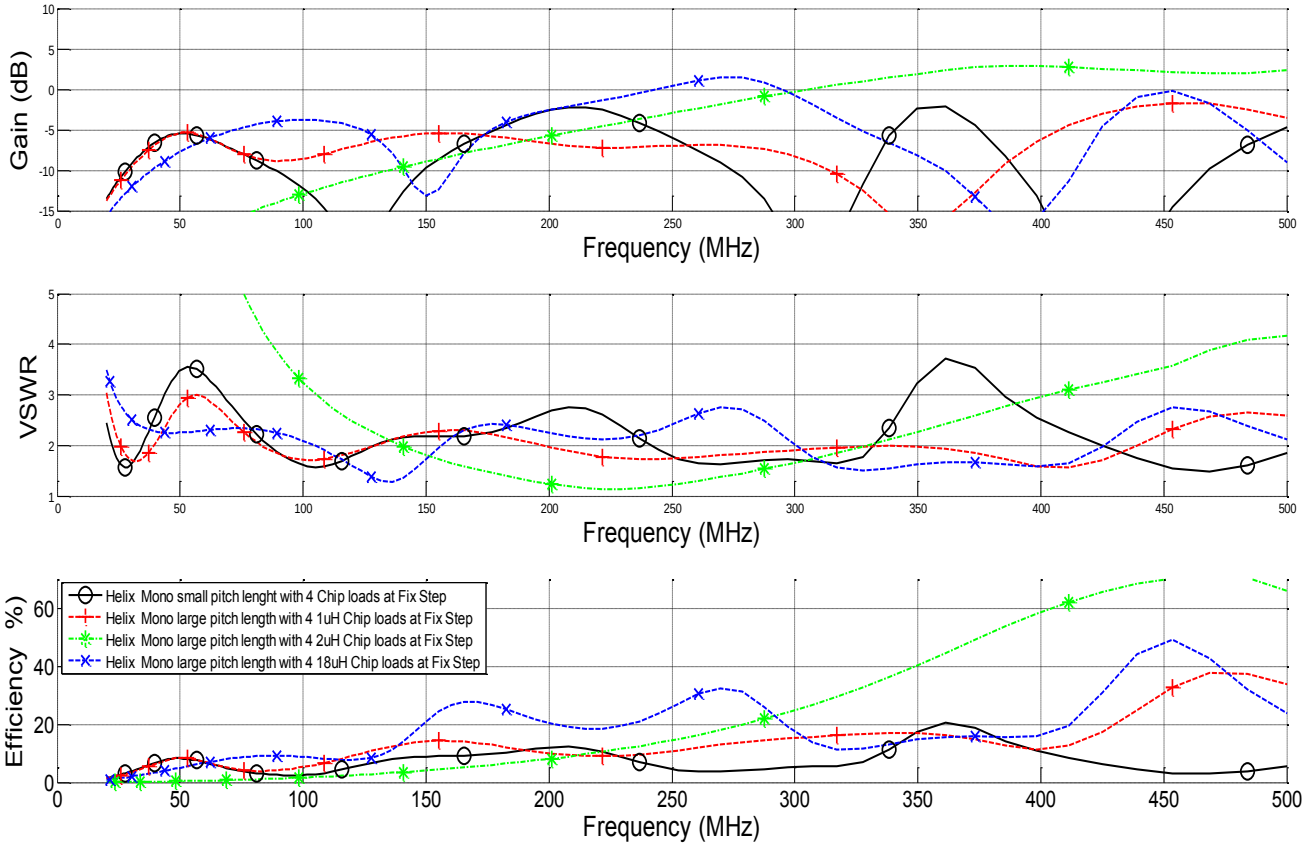

Figure 22: The gain and SWR of Helix monopole antenna with small and large pitch length and four 1, 2 and 18uH RL chip sections

3.3.3 Monopole antenna with a folded structure and RL chip sections at fixed locations

In this design the antenna is lengthened by another half of its maximum length by folding the antenna at the top (Figure 23). The antenna is still loaded with parallel inductors and resistors (Figure 24). Simulations were also performed using the same inductive loading used in the helix structured antenna simulations. Dimensions are: A = 300 mm, B = 600 mm, C = 900 mm and D = 1200 mm. The parallel resistor's resistance values were changed to values between 0 Ω and 1 kΩ to find the loading needed for a reflection coefficient lower than 0.48 and a gain higher than -10 dB.

The antenna's SWR was lower than 3 when 1 and 2 µH inductors were used in the RL chip sections, refer to Figure 25. The antenna's SWR increases above 3 at 20 MHz, reaching 2.8 at 175 MHz when an 18 µH inductor is used in the RL chip sections.

The folded antenna designs will not meet the specifications. Reason being that the antenna loaded with an 18 µH inductor will not meet the SWR specifications and the other two antennas do not meet gain specification. The antenna loaded with 1 and 2 µH inductors has a drop in gain at 400 MHz.

The folded antenna with 1 or 2 µH inductors would have been the ideal solution for it has stable SWR less than 3 across the bandwidth but does not contain a constant gain over its bandwidth.

The last topology to investigate is the monopole antenna loaded with RL chip sections.

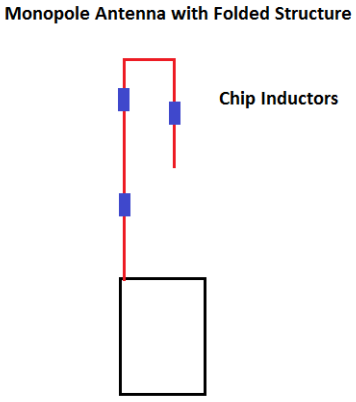

Figure 23: Folded monopole antenna with RL chip sections

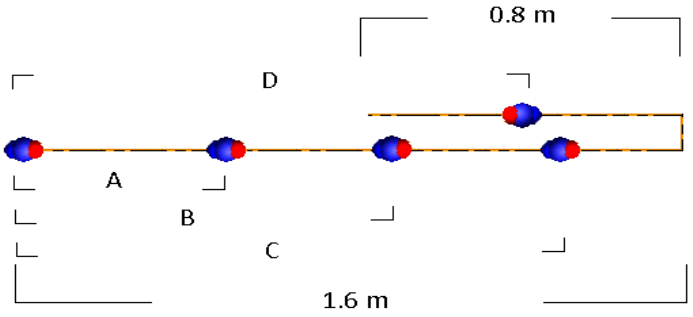

Figure 24: Folded monopole antenna dimensions

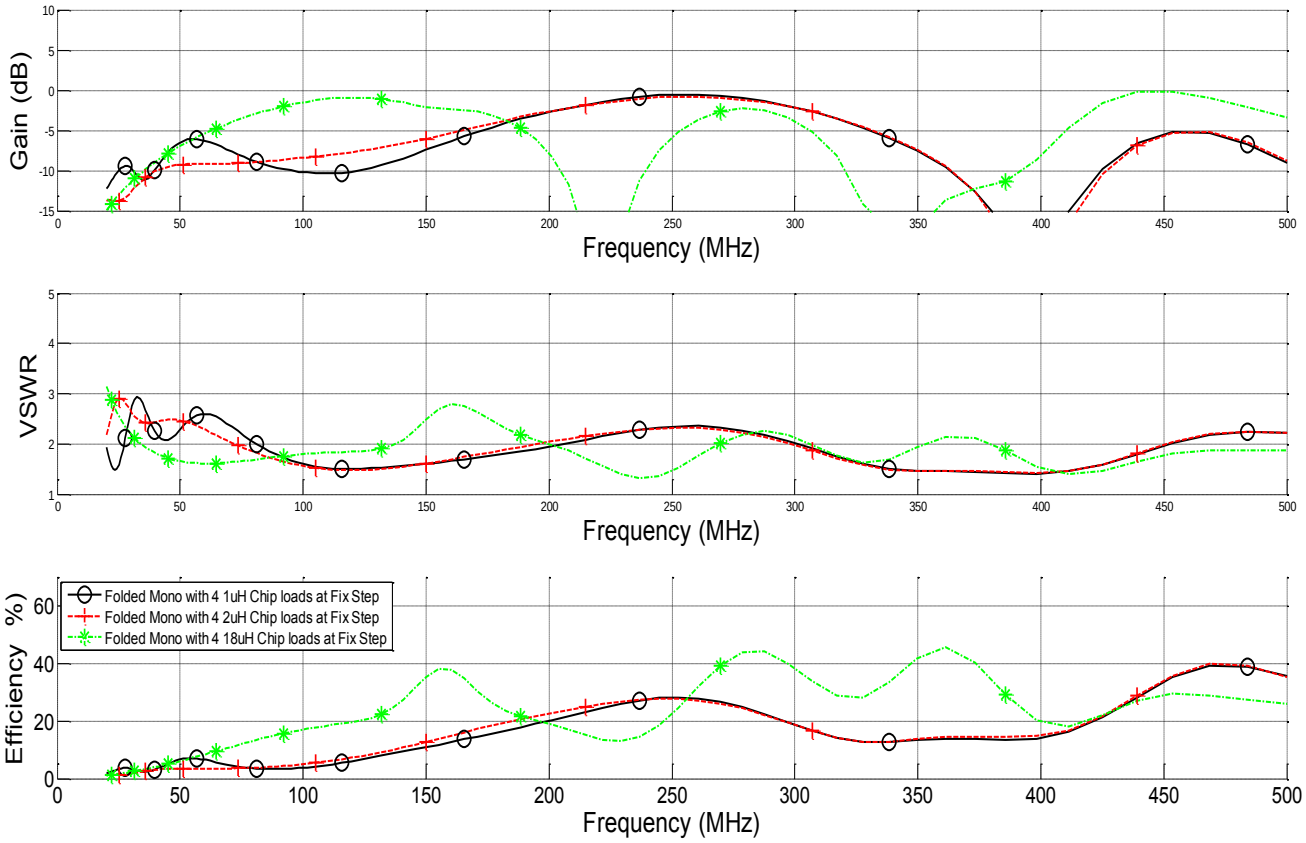

Figure 25: The gain and SWR of Folded monopole antenna with four 1, 2 and 18uH RL chip sections

3.3.4 Monopole antenna with RL chip sections at fixed locations

In this design the amount lumped elements were reduced from five (current amount on reference antenna) to four RL chip sections. The four RL chip sections were positioned 300mm from each other starting 300mm from the feed (refer Figure 26)

The RL chip sections were comprised of 1, 2 or 18 µH inductors in parallel with a resistor between 0Ω and 1kΩ. The parallel resistors' resistance values were changed to values between 0 Ω and 1 kΩ to find the loading needed for a reflection coefficient lower than 0.48 and a gain higher than -10 dB.

The monopole antenna with 18 µH inductors does not meet the SWR specifications between 20 MHz and 30 MHz for it still has a large capacitance at the low frequency. The antenna also does not meet the gain specification, being less than-14 dB, at 20 MHz and 500 MHz (refer to Figure 27).

The antenna meets the SWR and gain specifications when an inductor between 1 and 2 µH is used. The antenna with the 1 µH inductor has a 2 dB higher gain between 20 MHz and 250 MHz. The antenna's gain between 250 MHz and 500 MHz has a maximum difference of 2 dB lower than the antenna with the 2 µH inductor. The deciding factor of the inductance required lies in the SWR. When a 1 µH inductor is used the SWR of the antenna will increase to 3 at 20 MHz revealing that a 2 µH inductor is required.

The next step in the design proses would be to confirm the use of the right inductor by incorporating the inductor's S-parameters into the simulation and obtain the required resistor values.

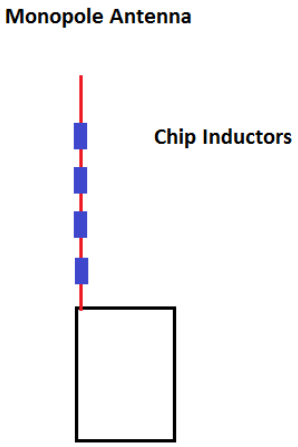

Figure 26: Monopole antenna with RL chip sections

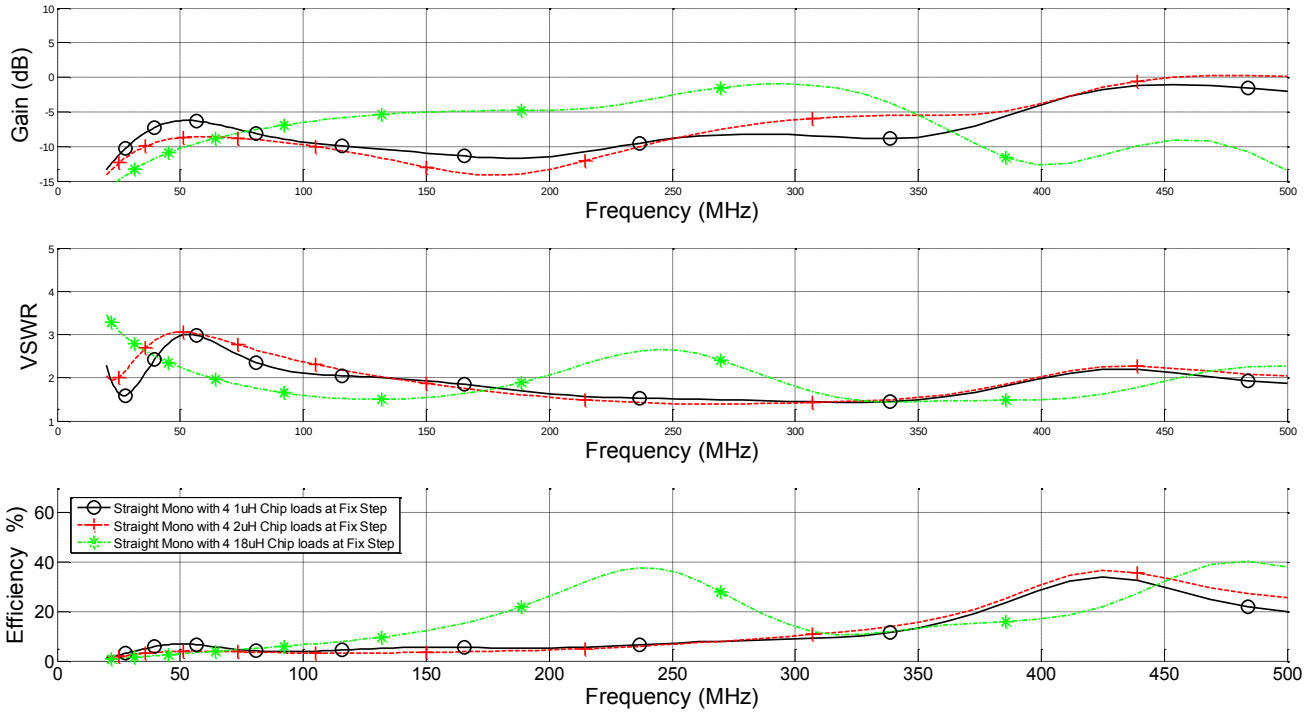

Figure 27: The gain and SWR of Monopole antenna with four 1, 2 and 18uH RL chip sections

3.4 Final monopole antenna containing chip inductors

3.4.1 Choice of inductors

The inductance values required can be obtained from a series combination of fixed ferrite inductors. A suitable ferrite material for the low frequency range is Perminvar, since its working frequency range is from 10 MHz to 200 MHz with a μ_i equal to 12. The problem with Perminvar would be the reduction in its permeability from 200 MHz upwards. This will cause the inductance to decrease from 200 MHz because of a change in permeability. The inductance is depend on the permeability, thus in this case adding less inductance to the antenna from 200 MHz upwards. Richard E Deasy and Cedar Rapids [7] advise the use of a chip inductor with a small cross-section for the upper frequency range.

The catalogues of a large inductor supplier, Coilcraft, were studied in the search for inductors which will work over the required frequency range, but the available 1 to 8 µH inductors mostly supply the inductance at frequencies lower than required. A compromise can be reached by adopting stacked combinations of either the 500 nH or the 560 nH inductors, which both work over the required bandwidth with acceptable resistance.

Referring to Figure 28 and Figure 29, the1008HT-R56T inductor with a 560 nH inductance was designed to be used for a bandwidth between 1 and 900 MHz, while the 10HTR56 has a higher than 590 nH inductance at 20 MHz, which increases to 1 µH at 475 MHz. The 08HTR50 model has a 490nH inductance, reaching 620 nH at 500 MHz and both inductors are experimented with numerically in FEKO.

Due to the strong deviation from ideal performance associated with ferrite inductors, it was imperative to optimize the design with the actual inductor's frequency characteristics. The inductors S-parameters were loaded from the supplier's web-page and added into the FEKO simulations in order to optimise the resistance that needs to be added. The addition of the supplied two-port inductance parameter S-parameters proved complicated in FEKO, but this was resolved by defining the second port as 'grounded'.

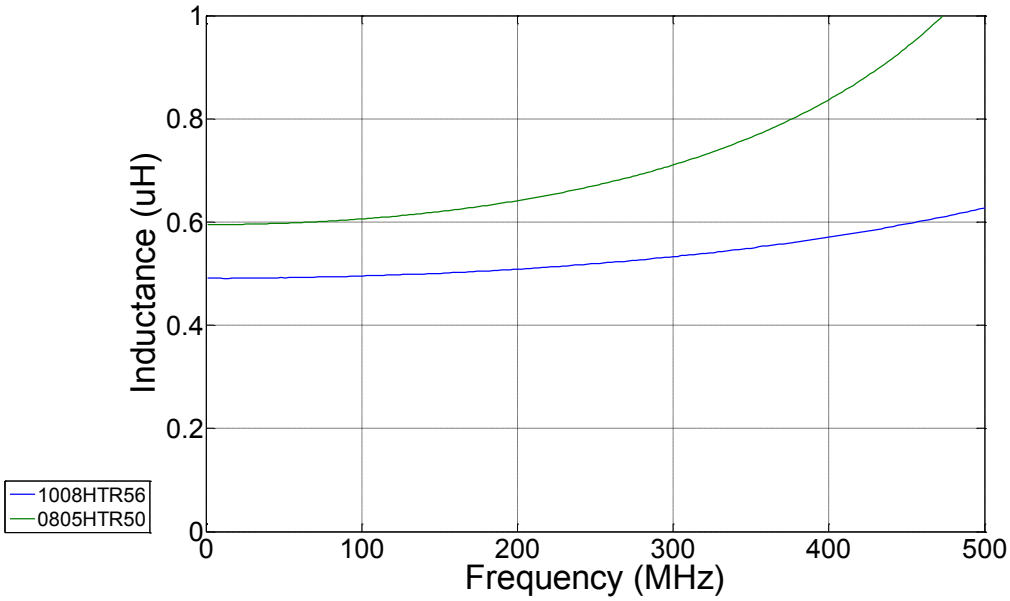

Figure 28: Inductance of 0805HTR50 (500nH) and 1008HTR56 (560nH) inductor from Coilcrafts

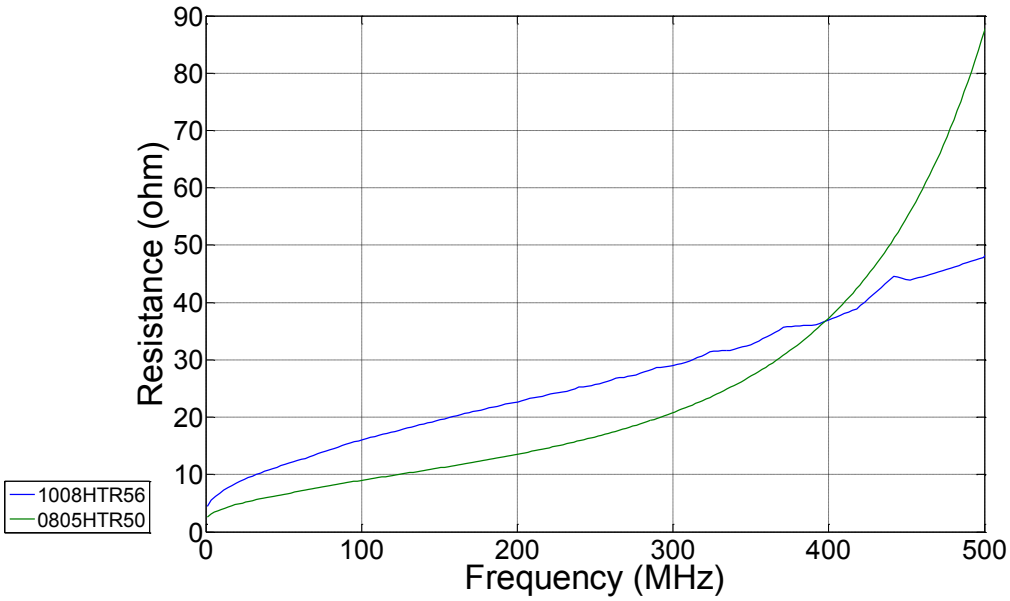

Figure 29: Resistance of 0805HTR50 (500nH) and 1008HTR56 (560nH) inductor from Coilcrafts

3.4.2 Inductor's frequency characteristics added to antenna model

The frequency characteristic data of the component which were going to be used, the 10HTR56 inductor, must be added in the form of S-parameters to the antenna model. The ideal antenna design, which fulfils the necessary specifications, was optimised with the component data to tune the necessary resistance which should be added. Any negative effects caused by the inductor can be tuned out when the S-parameters are introduced to the model.

The RL chip sections were constructed as shown in the schematic (Figure 30). Six inductors were placed in series with each other, with a parallel resistor. These RL chip sections were implemented in FEKO by placing six ports in series with each other on n wire segment and connecting a wire segment with a resistive load (Figure 31).

The measured S-parameters of the inductors for different frequencies are stored in a touchstone file and can be imported into FEKO as a general network. The measurements are those of a two port network and FEKO requires a one port network. The general network's first port is connected to the port which is located at the intended location (each of the six series ports) and the second port is short-circuited (Figure 32).

These RL chip sections are positioned at the locations shown in the antenna schematic (Figure 33). The only variable would be the magnitude of the parallel resistor connected to the six series inductors.

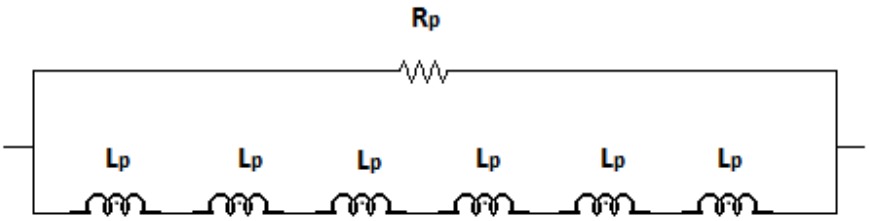

Figure 30: RL chip section schematic

Figure 31: RL chip section implementation in FEKO

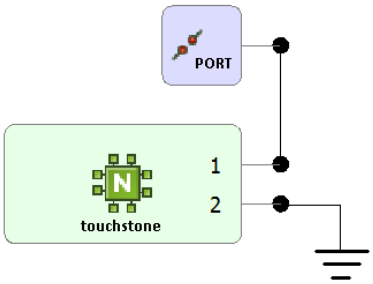

Figure 32: S-parameter imported into FEKO

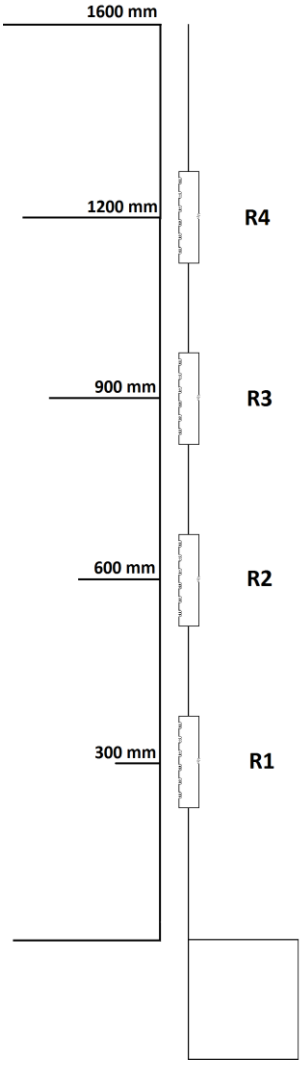

Figure 33: Antenna schematic implemented in FEKO

The FEKO model could be optimised after adding the 10HTR56 inductor's S-parameters. The required resistor values could be obtained for using atypical inductor. The optimisation showed that the following resistor values would allow the antenna to meet the SWR and gain specifications

Resistors in Figure 33:

R1. 270 Ω
R2. 200 Ω
R3. 560 Ω
R4. 680 Ω

Figure 32 depicts the SWR and gain of the antenna with the 10HTR56 inductors.

The 2 µH inductor was obtained by pressing four 10HTR56 inductors (560 nH) in series at each of the four RL chip sections. Figure 34 illustrates that the four series inductors, providing 2.2 µH, will still have a high SWR at 20 MHz and 500 MHz.

The inductance was increased by adding two additional inductors, forming six series 10HTR56 inductors. The antenna's gain is higher than -11 dB across the entire bandwidth reaching a maximum of 4 dB at 210 MHz (refer to Figure 34). The antenna has a standard wave ratio less than 2.5 over the bandwidth (20 MHz – 500 MHz).

The antenna's SWR boundary is reached at 20 MHz and 500 MHz when four series 10HTR56 (560 nH) inductors are placed in series to construct a 2 µH inductor. This problem is solved by using six series 10HTR56 inductors, raising the parallel inductance to 3.3 µH. This will deliver an antenna with a gain 3 dB higher with a similar SWR than the reference antenna.

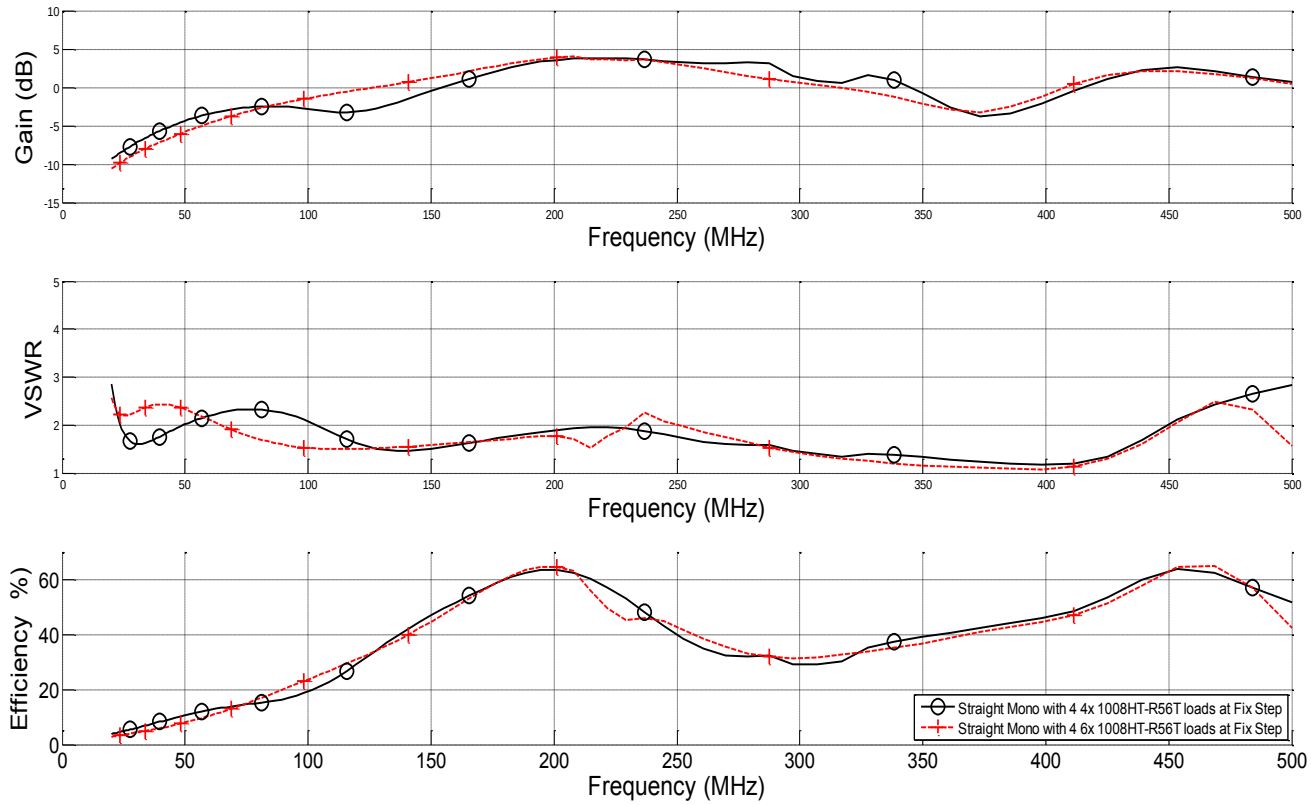

Figure 34: The gain and SWR of Finale antenna design

3.4.3 Final antenna design compared to reference antenna

The next phase will be to compare the new monopole antenna design with the reference antenna. The reference antenna's gain in SWR measurement data was extracted from its technical reference manual provided by Poynting. The gain and SWR of the two antennas are depicted in Figure 35. The gain of the new monopole antenna design with four RL chip sections, consisting of six series 560 nH inductors with a parallel resistor, exceeds the reference antenna's gain by 10 dB.

The monopole antenna design has a higher SWR, below three, than the reference antenna between 20 MHz and 275 MHz. The new design has lower SWR between 275 MHz and

500 MHz.

The new monopole antenna design will perform better than the reference antenna due to its higher gain. The next phase of the design process would be to build the new monopole antenna design containing the four RL chip sections with the six series 10HTR56 inductors.

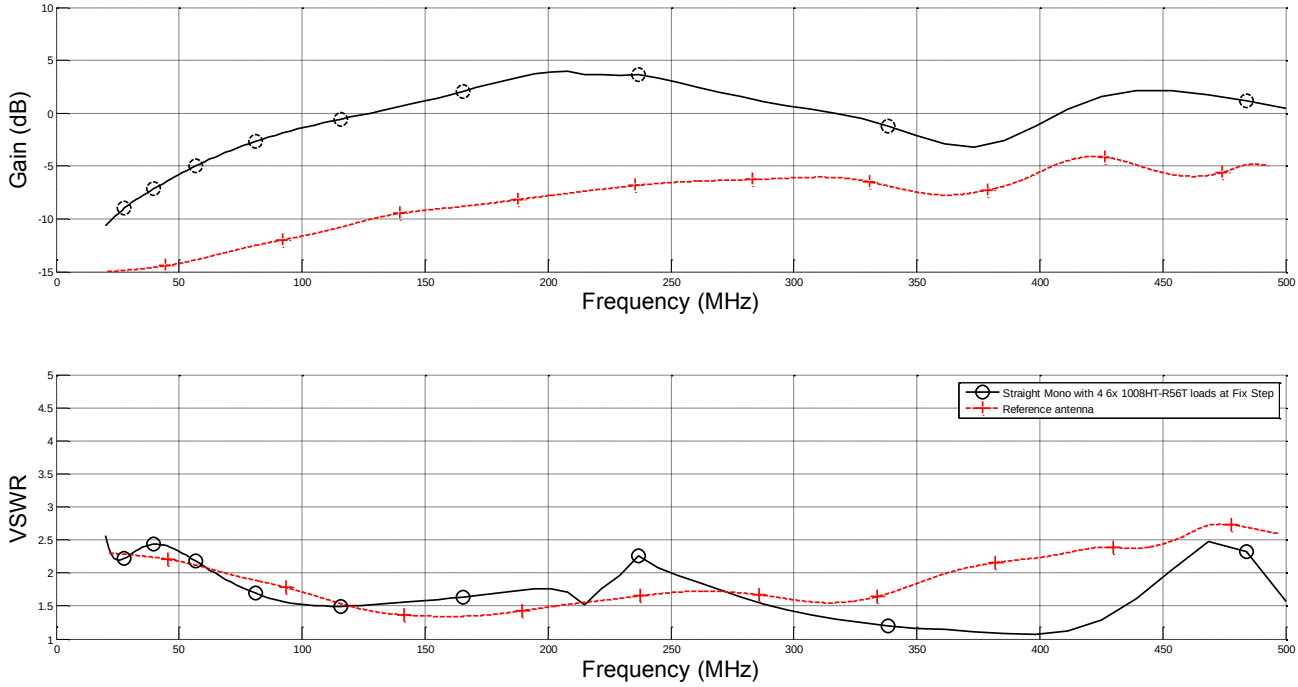

Figure 35: The gain and SWR of Final antenna design compared to Reference antenna [8]

3.4.4 The influence of a human body on the antenna

The next step is to analyse the effect a human body will have on the antenna since they would be in close proximity. This is done by adding a body, modelled as a box, with roughly the same dimensions of an average human body, 1.7m tall by 500 mm wide by 50mm deep, into the antenna model, Figure 36. The entire human body was set to the relative permittivity of 30.

Figure 37 shows that the body worsens the antenna's SWR at the low frequencies by adding extra capacitance to the impedance. The SWR has a value lower than 3 from 62 MHz upwards to 500 MHz.

The body's effect on the gain is partly advantageous: at 20 MHz it has a gain of -10.5 which rises to a maximum of 5 dB at 320 MHz and 7 dB at 450 MHz ending at 500 MHz at -2.5 dB, see Figure 35.

It is important to optimise the antenna with the body incorporated in the model. Techniques to reduce the body's influence on the antenna are left for a next phase of the work.

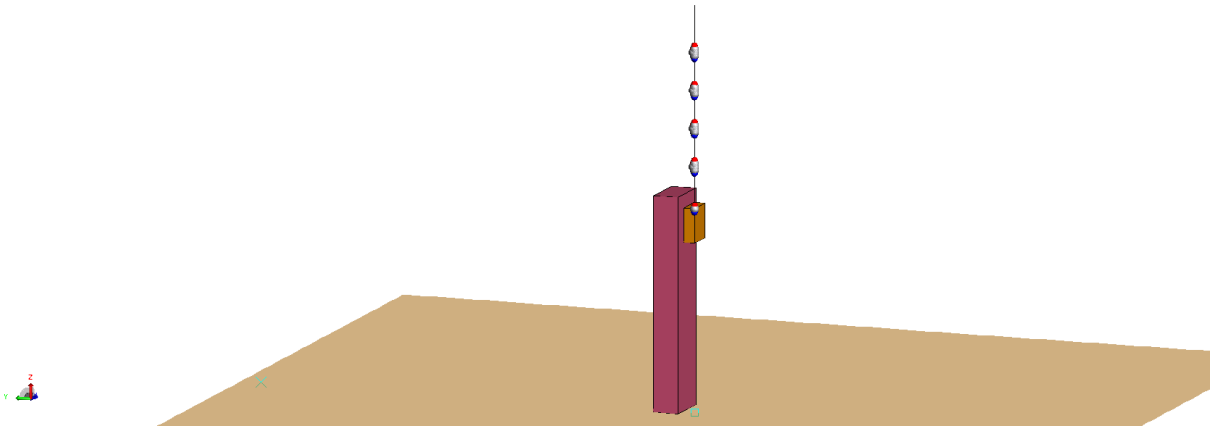

Figure 36: RL chip loaded monopole antenna with straight structure

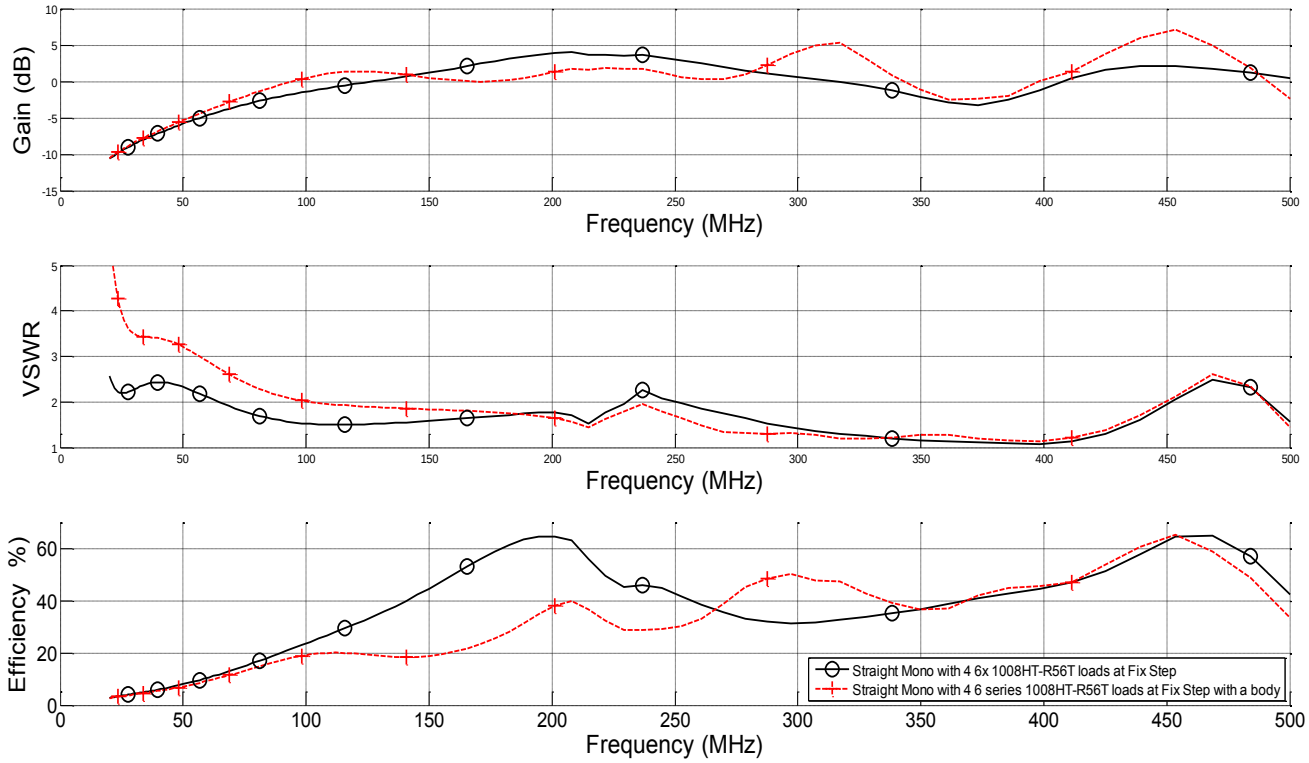

Figure 37: The gain and SWR of Final antenna design and Final design with a human body in close proximity

Chapter 4

4.1 Practical Measurements

Overview of measurements performed:

The antenna's reflection coefficient (S11) was measured and the near-fields were probed using a Rohde & Schwarz FSH6 network analyser (Appendix A.3). The network analyser was first calibrated using an open, short and load circuit to give an accurate measurement. The antenna was connected to the network analyser at its RF input with a coaxial cable. The antenna's reflection coefficient was measured for the following cases:

- The antenna position on a ground plane with and without a human body in close proximity (closer than a meter) to the antenna
- The antenna above the ground with a block of polystyrene with and without a wire extending two meters from the case (drag wire).

The influence of a human body on the antenna was tested by measuring the antenna's reflection coefficient with and without a body present whilst positioned on a ground plane. There were small discrepancies over the frequency range, with the most between 20 MHz and 300 MHz. All the measurements were compared to the simulation with the antenna mounted on the case at an offset, positioned above a ground plane**.**

The effect of the position at which the antenna is mounted on the case should be brought into account in the antenna model and simulated to compare with the measured results. Figure 38 shows the difference in the antenna's VSWR caused by the position at which the antenna is attached to the case. Simulations were performed with the antenna attached to the corner of the case and attached to the middle of a side top edge (at an offset).

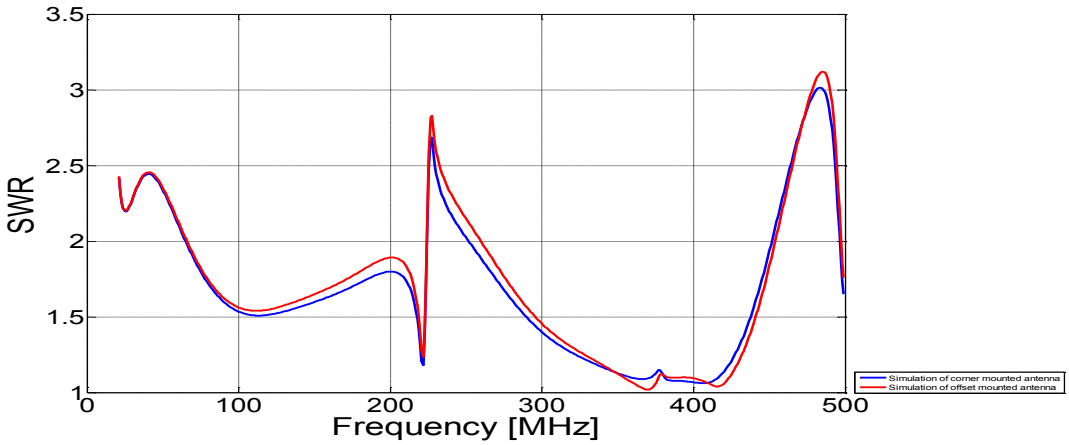

Figure 38: Simulated (red) VSWR of antenna mounted on corner (blue)

The antenna has a VSWR lower than 3:1 in all four cases, satisfying the required VSWR specification (Figure 39). The measurement with the antenna on the ground plane (green) should agree with that of the simulation (purple).

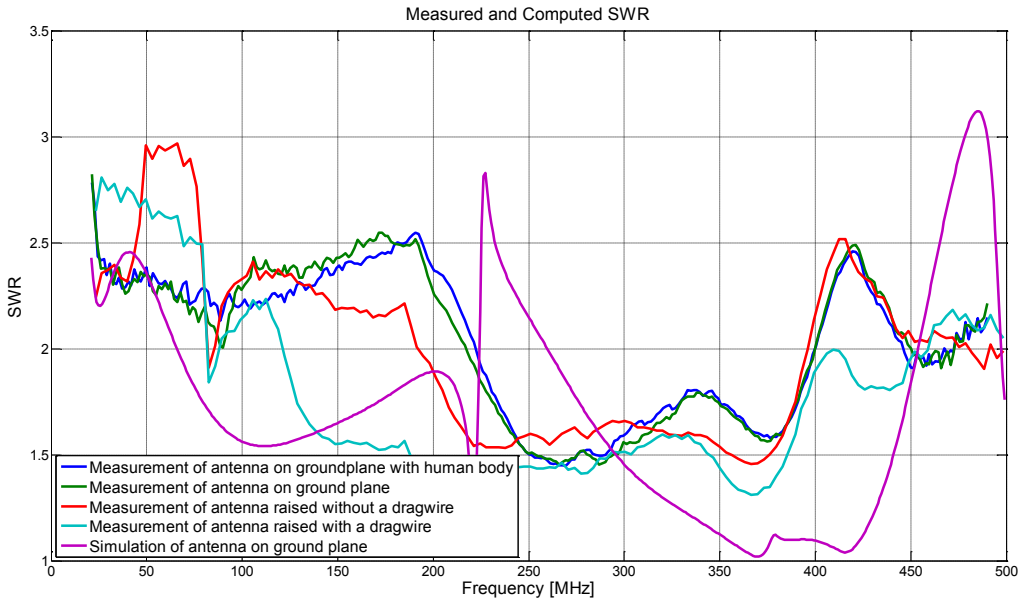

Figure 39: Measured and simulated VSWR results of antenna on a ground plane with (blue) and without (green) human body in close proximity, antenna raised above ground plane with (cyan) and without (red) a drag wire and the simulation of an antenna on a ground plain

Near-field measurements:

The near-field probe was positioned at three different heights which were set to a distance X equal to 0 and 300 mm above and below the antenna's connection point. The antenna's near-field was measured at a fixed distance X on the horizontal axis equal to 300 mm, refer to Figure 40 (b).

The Rohde & Schwarz FSH6 network analyser was calibrated with its open, short and load circuit in order to elude the effect of the transmission line (coaxial cable) on the phase measurement. The near-field probe has to be shaped as illustrated in figure 40 (a) in order to obtain an accurate reading. Extra currents were induced onto the wire affecting the measurements accuracy.

Each measurement is compared with its counterpart simulation. The near-field magnitude and phase was extracted and depicted on figure 41 and 42 below.

The measured near-field magnitude with the near-field probe at a height (X) equal to zero mm is similar to that of the simulation containing a small offset equal to 1 dB at the high frequency and 6 dB at 20MHz.

When the height (X) of the near-field probe is increased to 300 mm the offset increases to 2 dB and stays constant across the bandwidth. Only at the low frequency the measurement is 6 dB lower than the simulation

The offset between the near-field measurements and simulation fluctuate from positive to negative when the near-field probe height is decreased to 300mm below the antenna feed point. The offset fluctuates between 0 and 2 dB from 44 MHz towards 490 MHz with a larger near-field offset equal to 9 dB at 20 MHz

The phase component must also be compared to the simulations to verify the antenna's gain. The difference between the measured and simulated phase of the antenna decreases with an increase in height (X). The phase offset for the near-field probe 300 mm below the feed point is equal to 150° that decreases to 80° towards the feed point. The phase offset finally decreases to 40° when the near-field probe is raised to 300 mm above the feed point. The phase difference decreases from the maximum amount mentioned above to lower than 10°. The simulated and measured graphs follow a similar gradient where the main difference in the three measurements is an offset that decreases with an increase in frequency from 20 MHz.

The antennas far-field phase will be similar to the simulation's far-field calculations, with the only difference being an offset. It can be accepted that the antenna will have a gain equal to the simulated results.

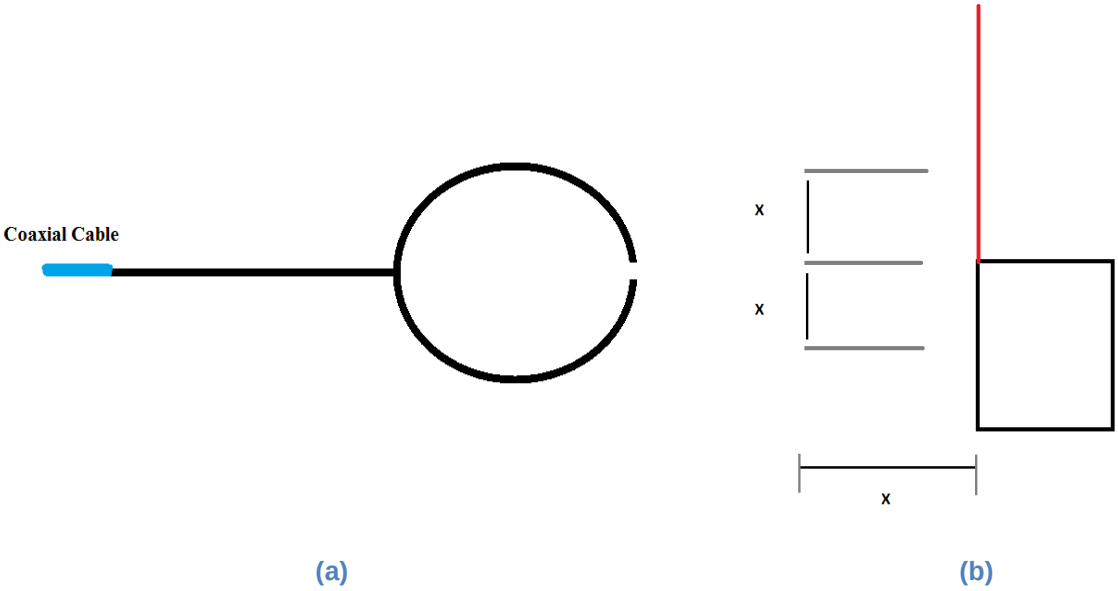

Figure 40: (a) Near-field measurement probe and (b) Measurements and simulation setup diagram.

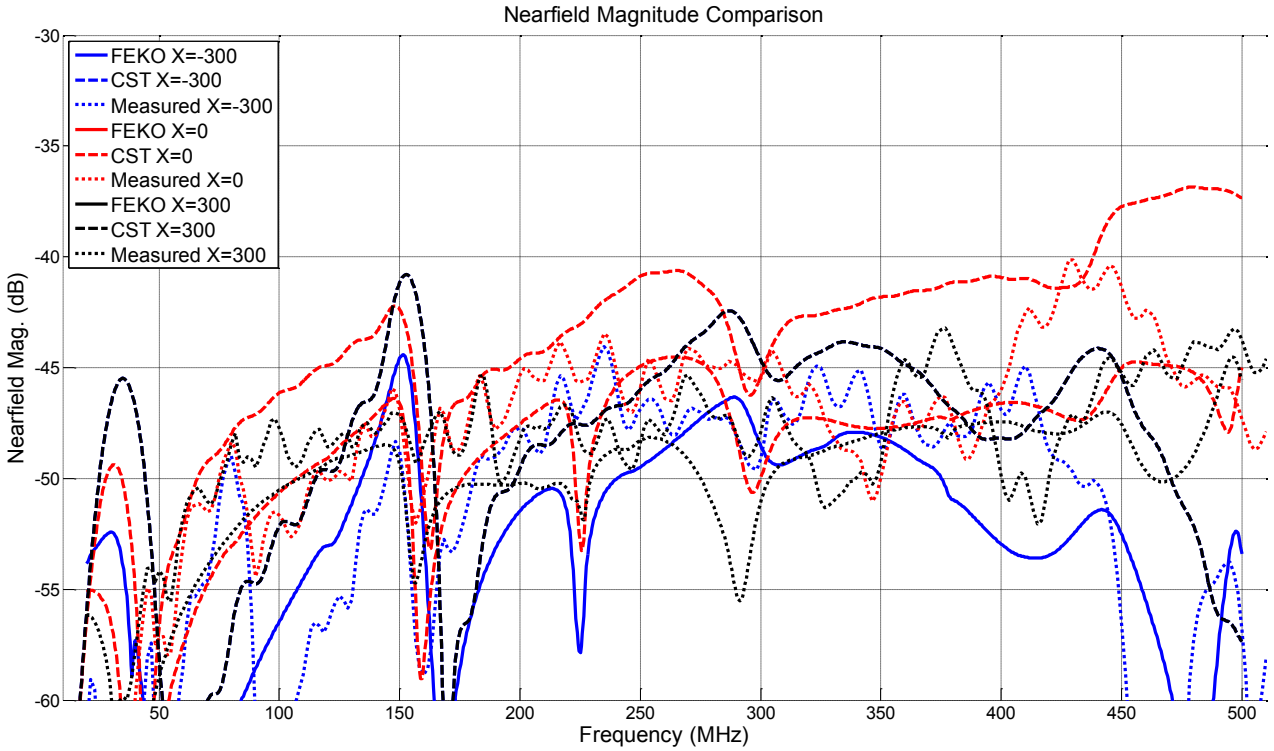

Figure 41: Near-field magnitude of measurement and simulation with X equal to 300mm above (Blue), below (Green) and adjacent (Black) to the feed of antenna.

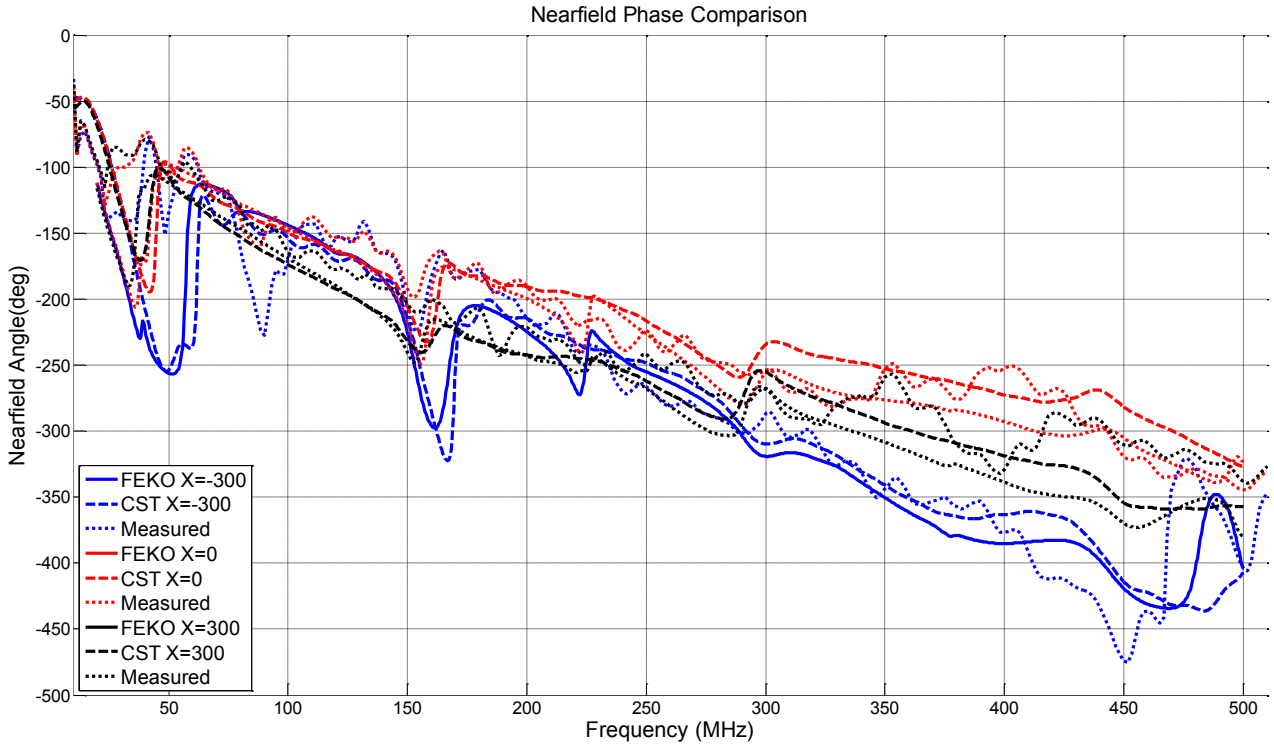

Figure 42: Near-field phase of measurement and simulation with X equal to 300mm above (Blue), below (Green) and adjacent (Black) to the feed of the antenna.

4.2 Final Antenna Configuration

Figure 43: Built loaded monopole on a ground plane

The antenna design which met all the design specifications was the 1008HT-560T inductive and resistive loaded monopole antenna. The next step was to construct the antenna and compare the measurements with the results of the simulations.

Referring to Figure A.1, the four loads on the antenna each contain six series 570 nH inductors supplying nominally 3420 nH per load. Each set of inductors has a parallel resistor with different resistance values connected to it. The distance between the feed and each load point is 300 mm. The wire section consists of copper foil tape with the loads connected and wrapped against a Perspex plastic rod to keep the copper wire vertical (shown in Figure 43).

A 6:1 impedance transformer was needed to transform the design reference impedance used in all the simulations from 300 Ω down to 50 Ω. The best available impedance transformer which will function in the working frequency range is a 4:1 Mini-Circuits impedance transformer. A larger reflection coefficient in relation to that of the simulation is to be expected, but this can be readily compensated mathematically from the measurements.

Another difference between the experimental implementation and the FEKO model is the antenna's attachment position on the case. In the simulation model it is positioned at one corner of the conducting case, whereas it is physically mounted in the middle of one side of top edge of the case. This should have only a minor effect, but a similar model should be used for the comparison.

An AN-type connector 'Panel Receptacle Jack' is used for the connection between the antenna and measuring equipment. The ADT4-6WT 4:1 transformer's primary pin is attached to the connector and the secondary pin to the antenna, with the primary and secondary DOT pins grounded to the case, as displayed in Figure 44.

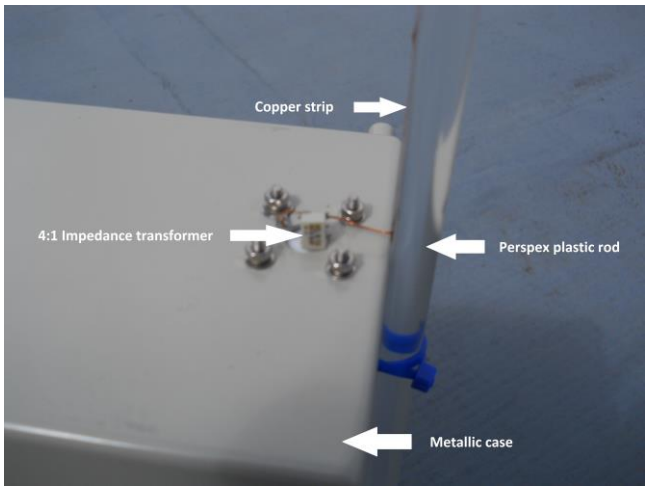

Figure 44: ADT4-6WT transformer and antenna mounted on case

4.3 Measurement equipment

The main measurements which need to be performed are those of the reflection coefficient and the gain. The reflection coefficient measurement was performed on top of the roof of a large building which contains enough conductive material (concrete reinforcing) to approximate a conductive ground plane.

The measuring equipment should be portable and must function in the required frequency range. The Rohde & Schwarz FSH6 Network Analyser, shown in Figure B.3, was used both to measure the reflection coefficient of the antenna and as a near-field probe.

4.4 Measurements performed

4.4.1 The reflection coefficient (S_{11})

S11 measurements were performed for four different situations: with the antenna box situated on the ground, on the ground with a human body in close proximity to it, mounted on a block of polystyrene with and without a wire extending from the case (drag wire).

The spectrum analyser was used to measure the antenna's reflection coefficient with a reference impedance of 200 Ω because of the 4:1 impedance transformer. These measurements needed to be transformed to a reference impedance equivalent to that of the simulation. Reference impedance equal to 300 Ω was used in the simulation. The antenna has to have nominal input impedance equal to 50 Ω, meaning a 6:1 impedance transformer would be needed. Since a 4:1 impedance transformer was necessary it was needed to re-normalise the measurements to a reference impedance of 75 Ω.

The phase delay through the N-type connector is significant at the higher frequencies. This was measured to be 40 mm, which will have an effect on the reflection coefficient's phase with a delay (Δ) double its length.

The phase will shift with:

$$\varphi = e^{j\frac{2\pi f}{c\Delta}}\Delta = 0.08 \text{ m} \quad [1]$$

The shift must be removed to view the correct reflection coefficient, and this is done by multiplying the measured reflection coefficient,Γ_v, for the different frequencies as follow:

$$\Gamma_v = Re^{j\theta} \quad [2]$$

To subtract the phase one can multiply equation [3] by equation [2] giving one the real reflection coefficient,Γ_r, in [4]:

$$\varphi_{-} = e^{-j\frac{2\pi f}{c\Delta}} \quad [3]$$

$$\Gamma_r = \Gamma_v . \varphi_{=Re^{j\theta}} . e^{-j\frac{2\pi f}{c\Delta}} \quad [4]$$

$$SWR = \frac{(1+|\Gamma|)}{(1-|\Gamma|)} \quad [5]$$

These mathematical instructions need to be performed to analyse and compare the antenna's frequency characteristics with those of the simulation.

Measurement cases

(a) Antenna on a ground plane

The antenna's VSWR was calculated by applying [5] to the measured reflection coefficient at different frequencies. The network analyser was used to measure the antenna's reflection coefficient in order to calculate its VSWR and phase; measuring the phase would be difficult using a VNA. The calculated VSWR is depicted in Figure 45 and compared to the VSWR of the simulation of the antenna on a ground plane.

The simulation's reference impedance must be set to 300 Ω to have a VSWR lower than 3, except at 475 MHz. The antenna's VSWR was measured at a reference impedance of 200 Ω because a 4:1 impedance transformer is used. The VSWR is mathematically scaled to a reference impedance of 300 Ω to compare with that of the simulation. The antenna's VSWR is lower than 3 across the entire frequency range with reference impedance equal to 300Ω.

The input impedance of the antenna with the 4:1 transformer is equal to 150 Ω, where the simulation predicted an impedance of 300 Ω (Figure 46). The antenna has a maximum VSWR equal to 2.8 at 20 MHz and which is lower than 2.5 between 450 MHz and 500 MHz. This simulation predicted a rapid increase to higher than 3.

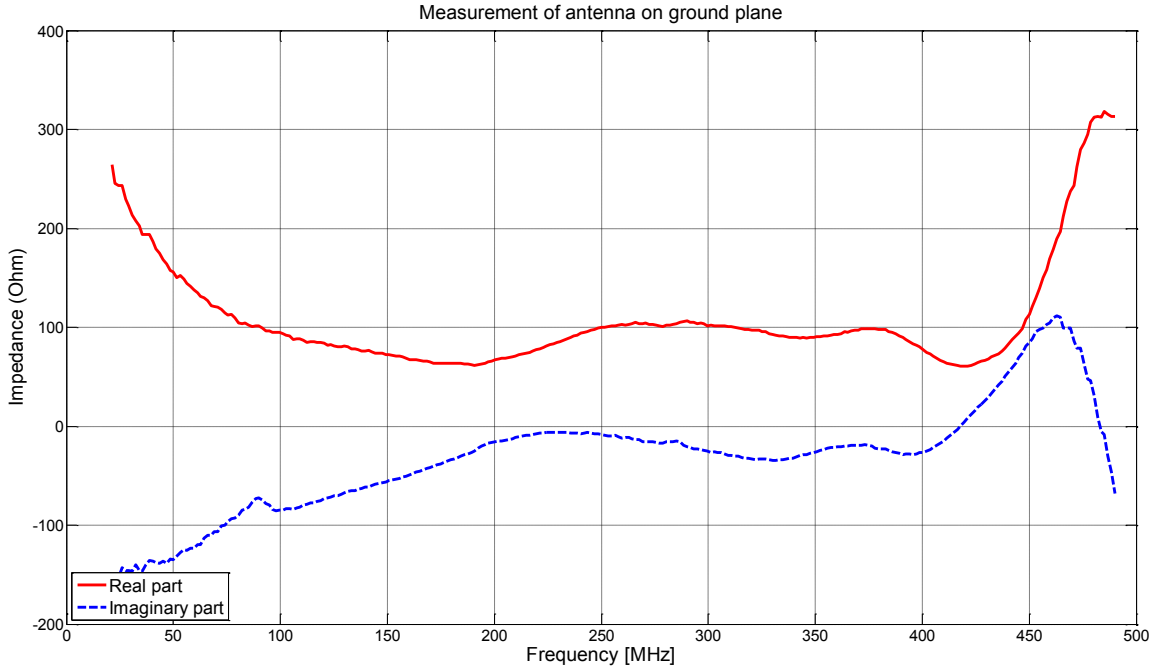

Figure 45: Measured impedance of antenna on a ground plane, Real part (red) Imaginary part (blue)

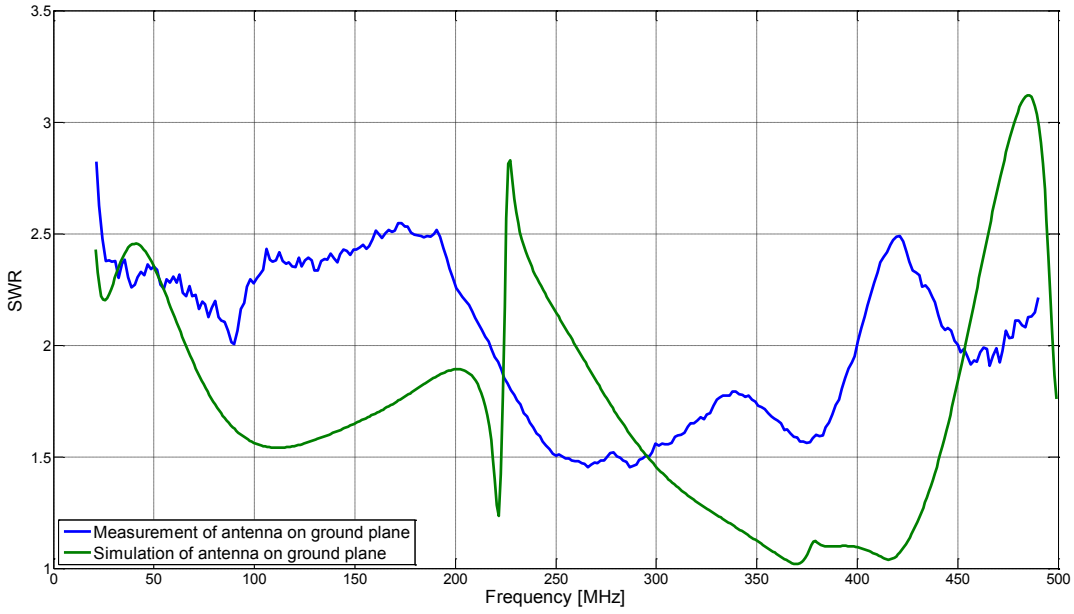

Figure 46: Measured VSWR of antenna on a ground plane (blue) compared to Simulation (green)

(b) Antenna on a ground plane with human body

A human body was placed in close proximity to the antenna when the antenna's reflection coefficient was measured. Figure 47 shows that the antenna has a VSWR of lower than 3, with a maximum of 2.8 at 20 MHz and an average of lower than 2.5.

Comparing the VSWR of the antenna with and without the presence of a human body, (Figure 48) it seems that the body had minor effects on the antenna and less than predicted by simulations (Figure 37). The only difference between the two cases' VSWR in figure 38 appears between 100 MHz and 175 MHz, where the human body lowers the VSWR slightly.

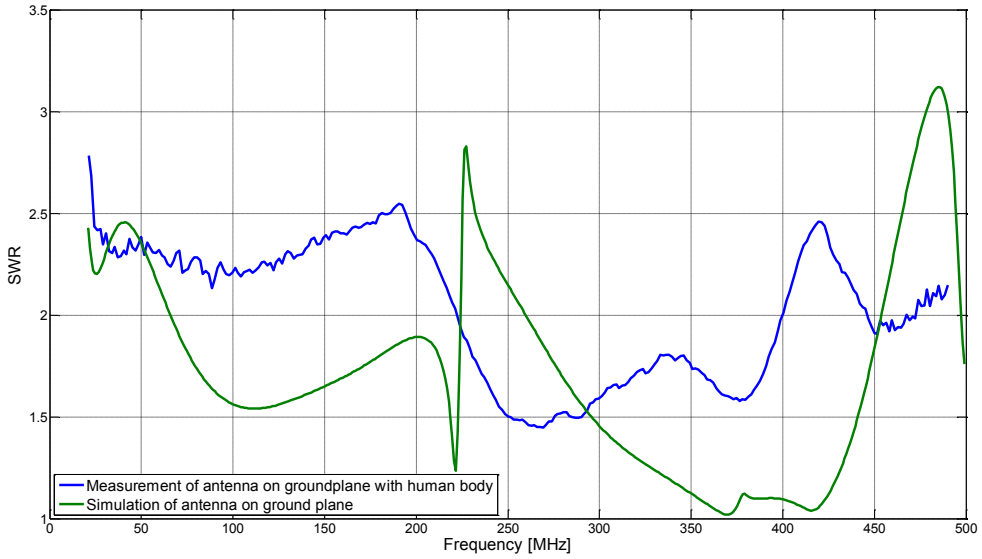

Figure 47: Measured (blue) and simulated results (green) of the VSWR of antenna on a ground plane with a human body in close proximity.

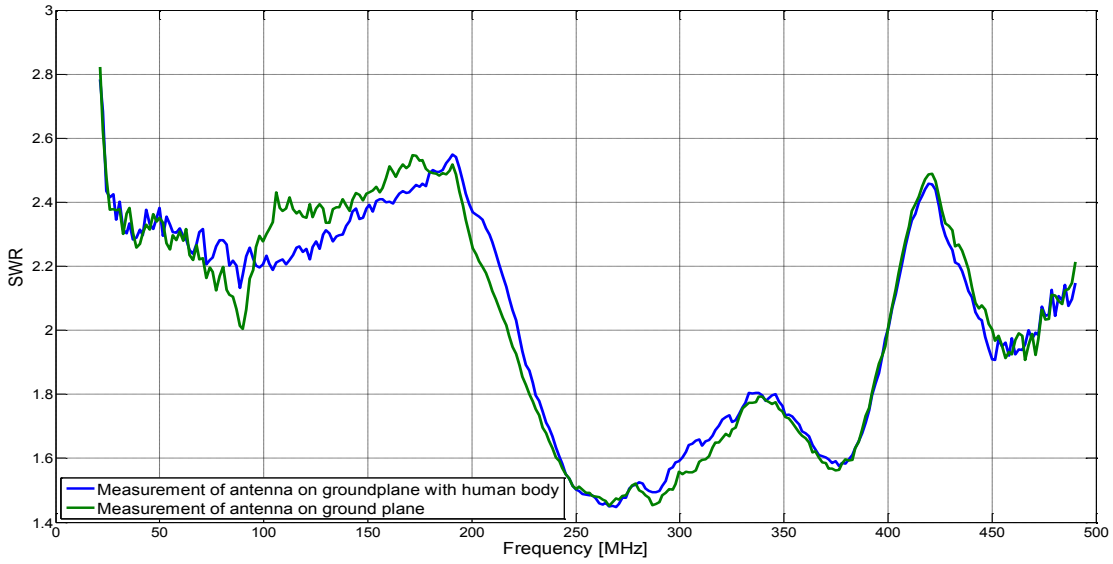

Figure 48: Measured VSWR of antenna on a ground plane with (blue) and without (green) human body in close proximity

(c) Antenna raised without a drag wire

In this measurement the antenna was placed on top of a polystyrene block to achieve a 1 m elevation. The effect of the distance between the case and the ground plane was tested with this measurement. The maximum VSWR occurs between 50 MHz and 75 MHz, as depicted in Figure 49. The antenna's VSWR is mostly lower than 2.5 over the rest of the bandwidth.

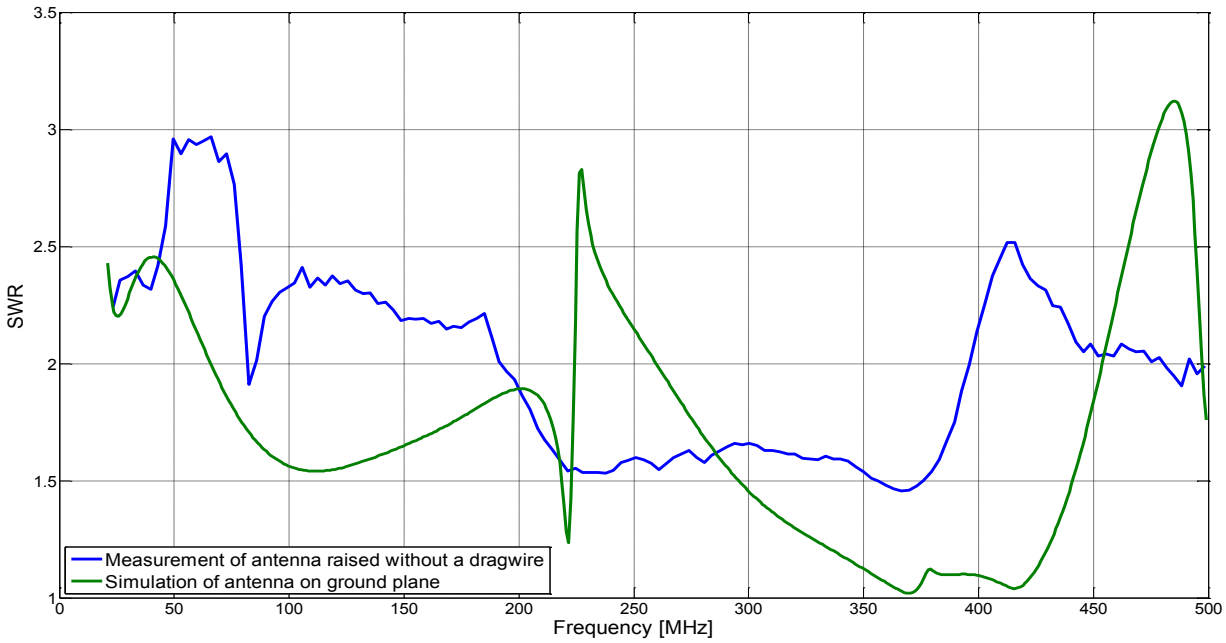

Figure 49: Measured VSWR of an antenna raised above a ground plane without a drag wire (blue) compared to the simulation of the antenna mounted at an offset on the case (green)

The main difference between the antennas situated on the ground and those raised 1 m above the ground, occurs at 20 MHz. Referring to Figure 50, where the VSWR of antenna on the ground plane is 2.8 and for the raised antenna is 2.2. The raised antenna has a better VSWR over the bandwidth, except between 40 MHz and 80 MHz.

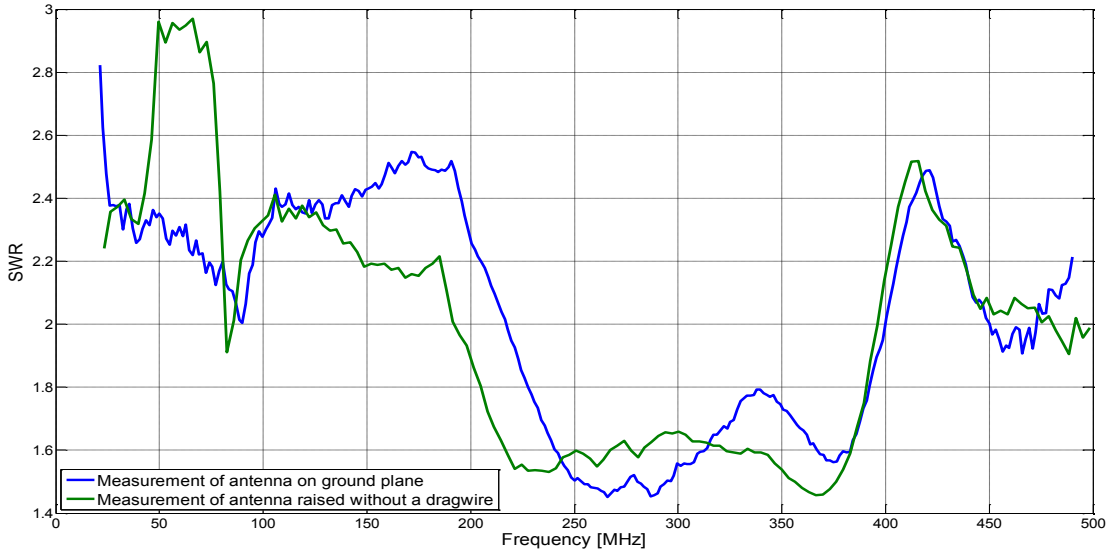

Figure 50: Measured VSWR of antenna raised above a ground plane (green) and an antenna on a ground plane (blue)

(d) Antenna raised with a drag wire

In this measurement the antenna was place on a polystyrene block to give an elevation of 1 m and a 2 m long wire was connected to the case. The antenna still has a high VSWR at the low frequencies, with a maximum of 2.8 at 26 MHz, (Figure 51).

The VSWR is lowered over the bandwidth by the addition of the drag wire, except between 20 MHz and 46 MHz and at the high frequency between 460 MHz and 500 MHz (Figure 52).

The big difference in the VSWR is between 125 MHz and 225 MHz and 400 MHz and 450 MHz. This is because the drag wire adds more resistance to the antenna's impedance, (Figure 53). A small capacitance is also added but the imaginary part of the antenna's impedance is virtually the same.

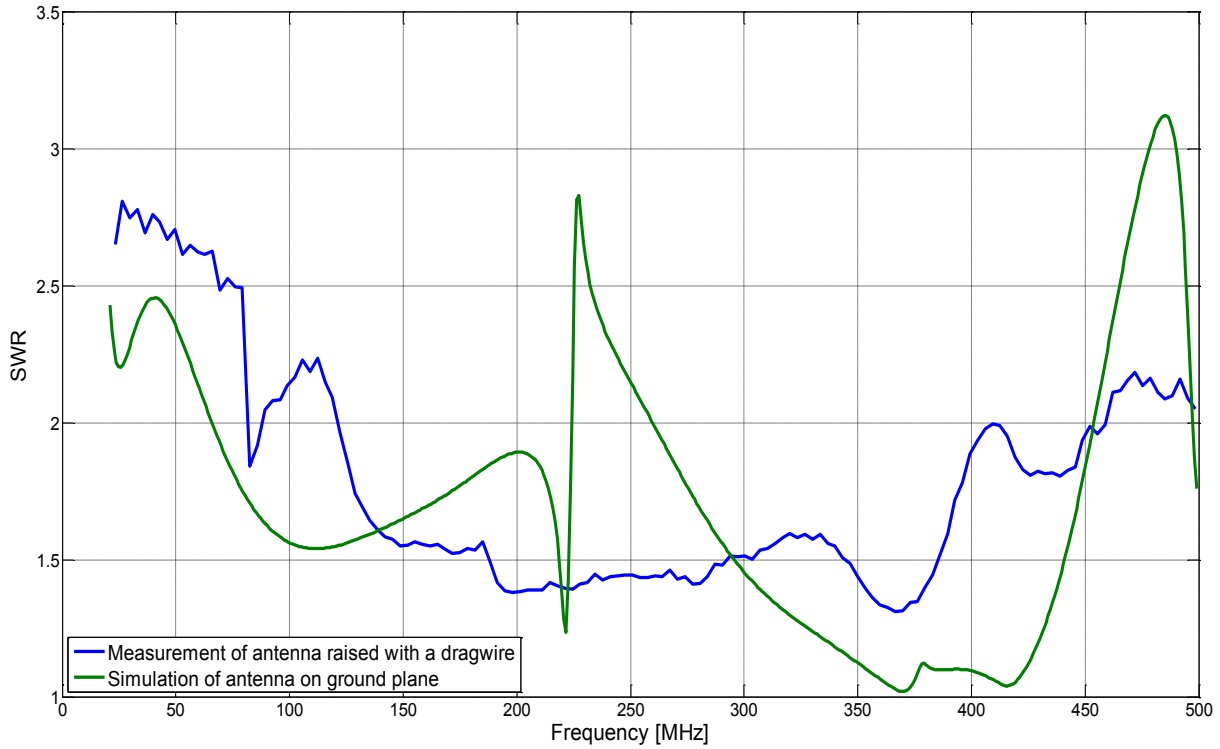

Figure 52: Measured VSWR of a raised antenna with a drag wire (blue) compared to the simulation of the antenna mounted offset on the case (green)

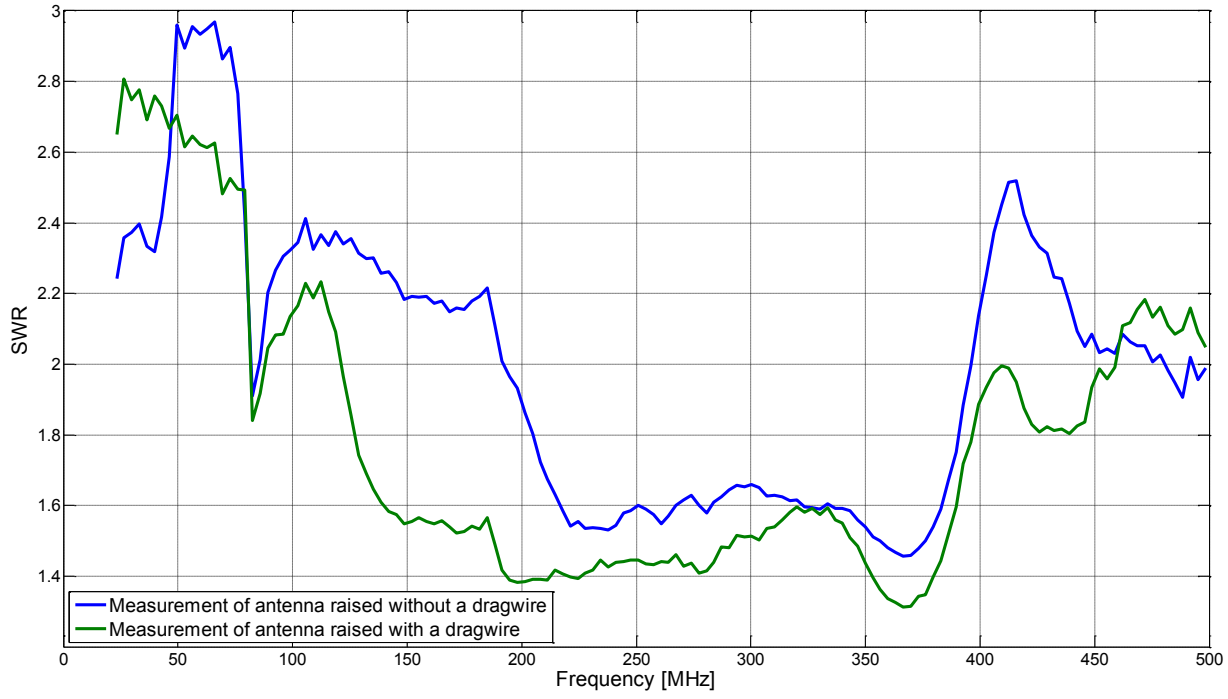

Figure 51: Measured VSWR of raised antennas with (green) and without (blue) drag wire

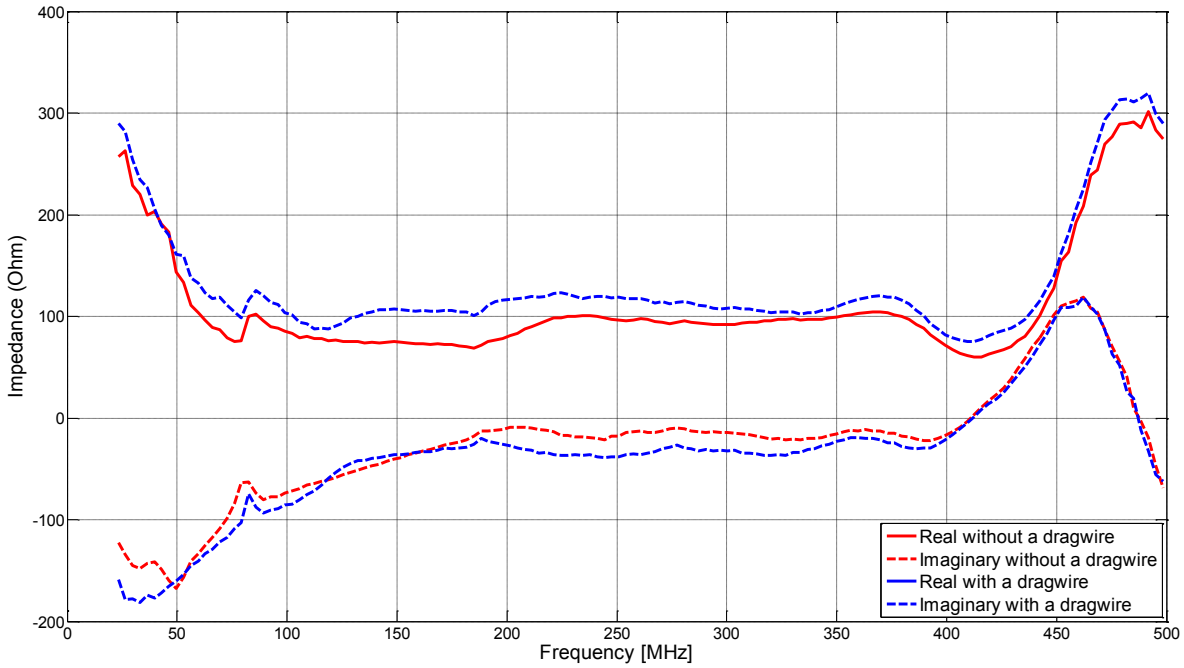

Figure 53: Measured impedance of raised antennas with (blue) and without (red) drag wire Real part (Solid line), Imaginary part (stipple line)

4.4.2 The forward transmission coefficient (S_{21}) - near-field

This measurement was performed using the same spectrum analyser used in the previous section but with a different setup. A near-field probe was constructed to the form depicted in Figure 36 in order to avoid interference from other induced currents on the wire connected to the coaxial cable. The probe has a diameter equal to 90 mm and the length of the connecting wire is 300mm.

The measurement could be performed after the network analyser was calibrated for the different lengths of coaxial cables used to connect the probe and antenna to the network analyser. The network analyser uses the two measurements to determine the antenna's near-field for each frequency.

The network analyser firstly needed to be calibrated with the different feed lines (coaxial cables) to get precise readings. One could then take sets of measurement with the probe at three different heights at a constant distance away from the antenna; refer to Figure 34. The probe was placed 300 mm across the position at which the antenna was attached to the case. The probe was lifted and lowered by 300 mm at the same distance from the antenna, to compare the near-field measurements from different locations.

The goal is to measure the S_{21} parameters to get the magnitude and phase of the antenna's near-field and compare it to the equivalent simulation. If the results concur then the practical antenna will have the same performance, gain and efficiency, as those of the simulations.

4.4.2.1 Near-field Magnitude:

Each measurement is compared with its counterpart FEKO and CST simulation. The near-field magnitude and phase was extracted and displayed on the graphs depicted below. The S-parameters imported into FEKO could not be used in CST, forcing the model to use ideal chip inductors.

(a) Near-field probe height (X) equal to 0mm:

When the measurement taken with X equal to zero mm (where antenna connects to case) it was observed that the near-field magnitude of the measurement was similar to that of the simulations. The maximum difference in the magnitude between the FEKO simulation and the measurement (refer to Figure 54) is at 428 MHz, where the measurement is 7 dB higher than the simulation.

When comparing the CST simulation to the measurement, the maximum difference increases to 10 dB higher than the measurement at 346 MHz. The measurement result does not decrease far below the FEKO results, mainly varying between the FEKO and CST results.

The dips and spikes in the CST model's near-field is the presence of a reflection from the ground plane. The frequencies affected by the reflection are dependant on the antenna's height from the ground plane.

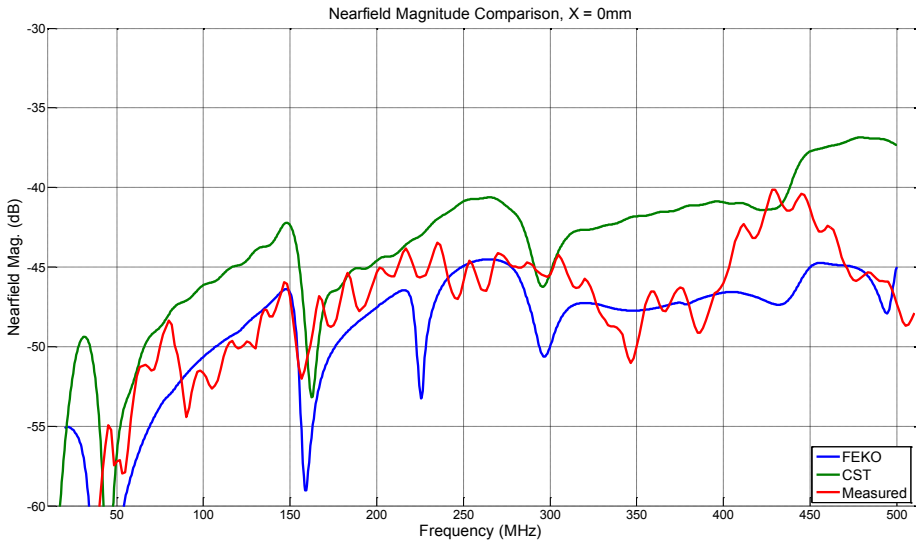

Figure 54: Near-field Magnitude of measurement and simulation with X equal to 0mm above

(b) Near-field probe height (X) equal to 300mm above feed point:

When the measurement was taken at a height of 300 mm, an improvement was observed when comparing the measurement to its simulations (refer to Figure 55). The measurement equals is OR is 2 dB higher than the simulation between 35 MHz and 242 MHz. The difference between the FEKO simulation and the measurement reaches a minimum equal to 5 dB at 415 MHz. The measurement is higher than the CST and FEKO results between 48 MHz and 128 MHz, with a difference of 5 dB with the FEKO

results and 8 dB with CST. The biggest near-field difference between the FEKO and the measurement result is equal to 7 dB at 291 MHz.

The largest difference between the CST simulation and the measurements is at 169 MHz. CST calculates a near-field 20 dB lower than what was measured. The CST simulation's near-field also increased to 14 dB higher than the measurement, at 35 MHz. The rapid increase and decrease in the near-field at 35 MHz and 169 MHz is caused by the reflection from the ground plane.

The measurement fluctuates between the FEKO and CST simulation, in the measurement with the probe at a height equal to 0 mm.

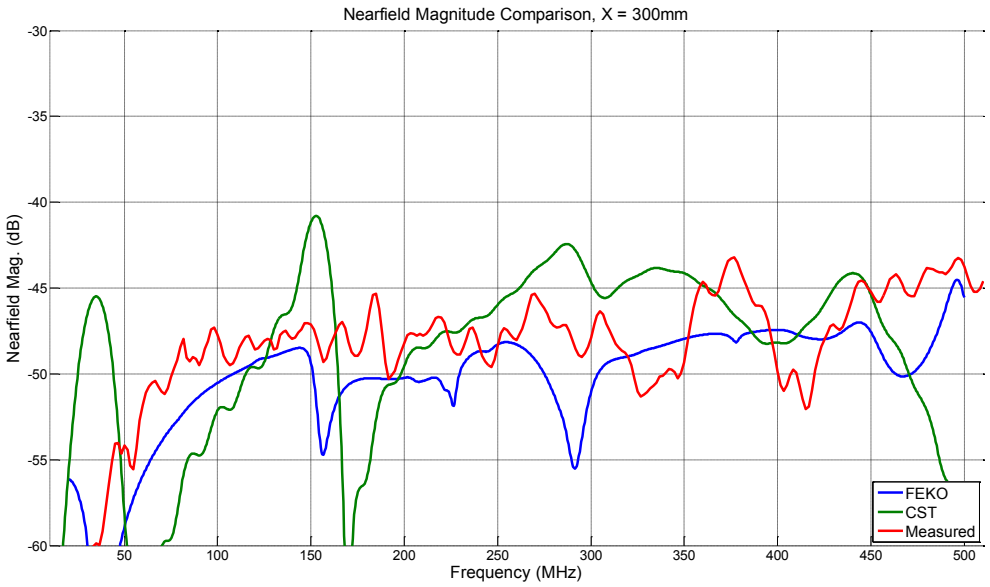

Figure 55: Near-field Magnitude of measurement and simulation with X equal to 300mm above

(c) Near-field probe height (X) equal to 300mm below feed point:

The comparison between the measurement and simulations where the near-field probe was lowered by 300 mm is displayed in Figure 56. The largest near-field difference between the CST simulation and the measurement is at 35 and 169 MHz. The CST result at 35 MHz is 20 dB higher than the measurement. The measurement is 17 dB higher than the CST simulation at 169 MHz.

The Measurement is 7 dB higher than the FEKO simulation at 292 MHz, remaining mostly above the FEKO simulation across the bandwidth.

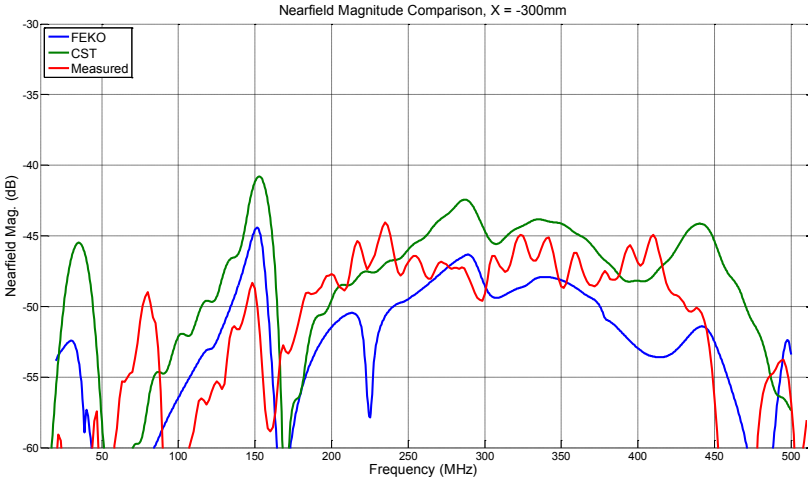

Figure 56: Near-field Magnitude of measurement and simulation with X equal to 300mm below

Near-field Phase:

A comparison was performed between the near-field's phase for the simulation and measurement case. The three near-field measurement cases were compared to their counterpart simulation case to validate that the antenna has the calculated far-field magnitude and phase.

(a) Near-field phase comparison at X equal to 0mm

The antenna's phase measurement results at a height equal to zero mm are illustrated in Figure 57. The measured phase has a maximum difference equal to 100° and 120° between 26 MHz and 46 MHz. The measurement has a larger phase between 100 MHz and 166 MHz and in the higher frequencies between 386 MHz and 426 MHz. The measurement follows a similar gradient to that of the simulation. It can be accepted that the antenna's phase will be equal to that of the simulation.

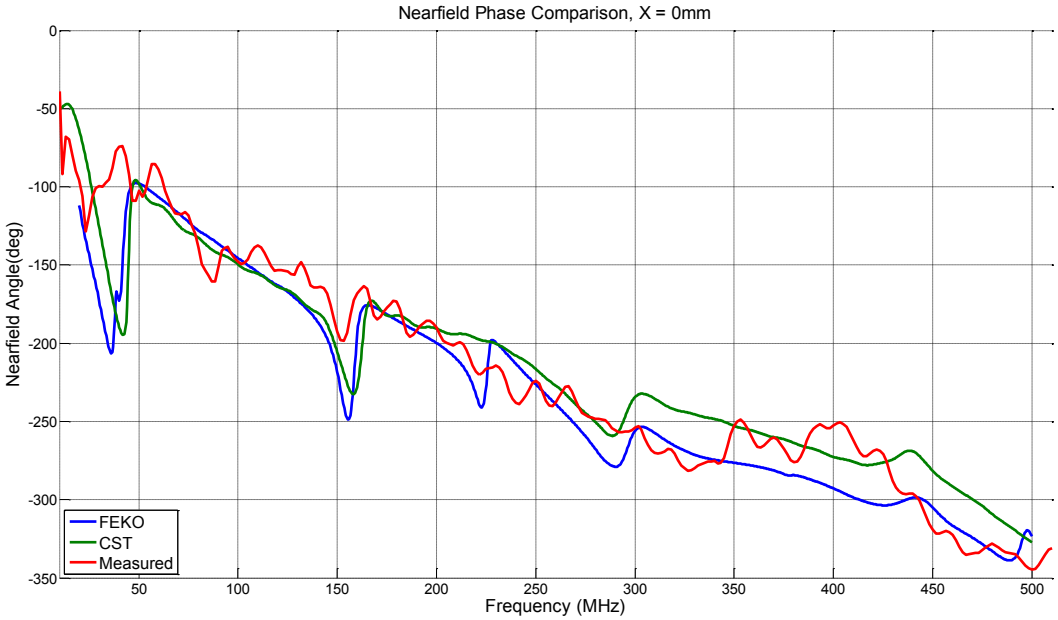

Figure 57: Near-field Phase of measurement and simulation with X equal to 0mm

(b) Near-field phase comparison at X equal to 300mm above attachment point

From 25 MHz to 500 MHz, the antenna's measured near-field phase remains mostly above the FEKO and CST simulation. The measurement decreases below the CST results, becoming equal to the FEKO results between 288 MHz and 330 MHz, as Figure 58 illustrates.

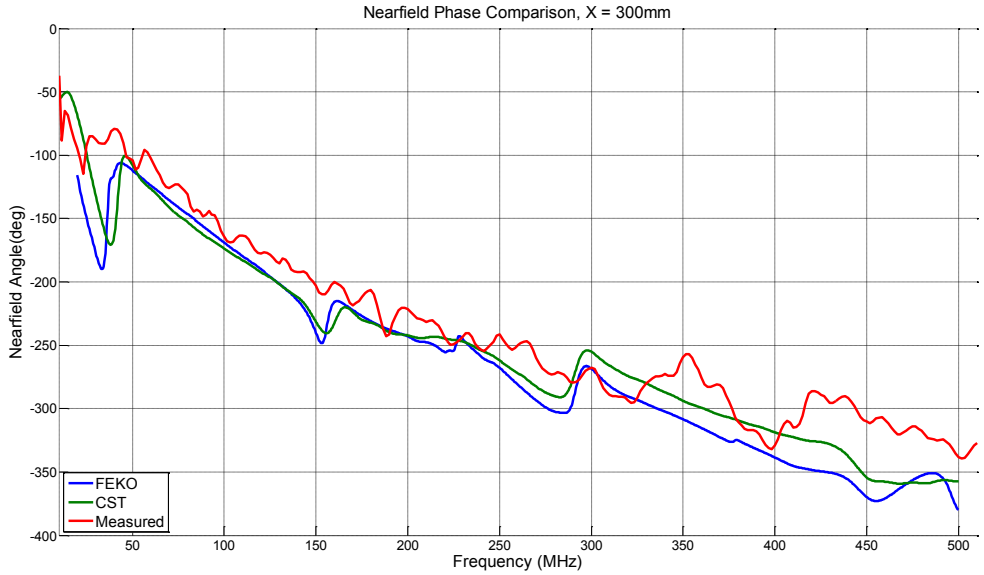

Figure 58: Near-field Phase of measurement and simulation with X equal to 300mm above

(c) Near-field phase comparison at X equal to 300mm below attachment point

The last measurement that needs to be compared to its simulated counterpart is where the near-field probe is positioned 300mm below the attachment point of the antenna on the case (refer to Figure 59).

The results of the measurement and simulations between 185 MHz and 410 MHz are similar. The biggest difference is at 41 MHz where the measurement is 28° higher than CST and 43° higher than FEKO. This is caused by the reflection of the ground plane.

The comparison between the simulations and the measurement in the three cases confirms that the measured antenna and both antenna simulations have similar frequency characteristics. The antenna will thus meet the design requirements.

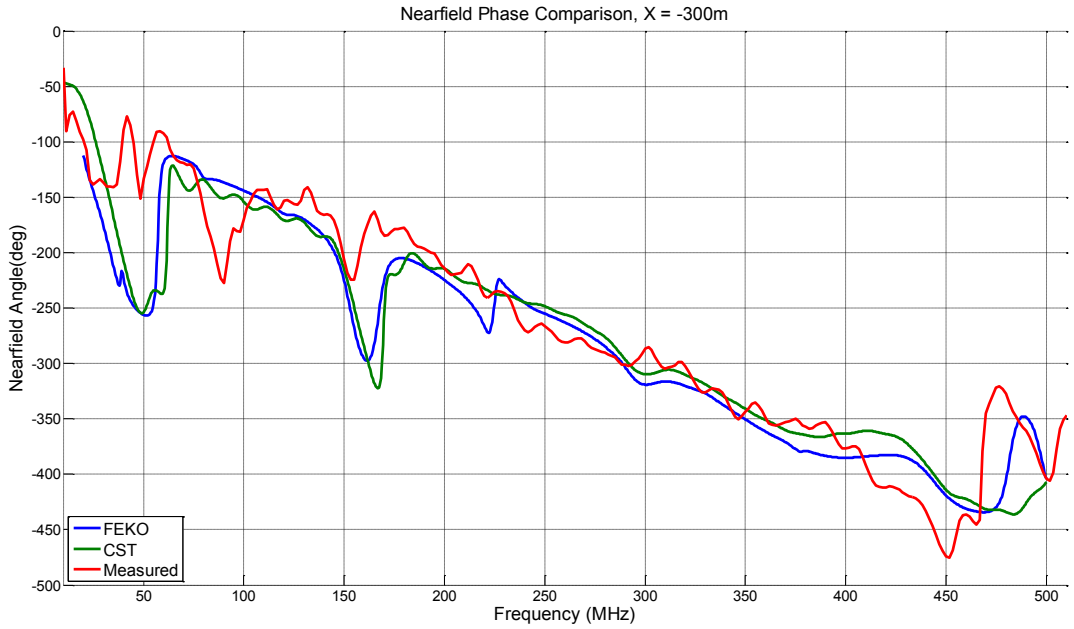

Figure 59: Near-field Phase of measurement and simulation with X equal to 300mm below

4.4.3 Power handling

$$I(rms) = \sqrt{\frac{2P}{R}} \qquad [5]$$

With the use of [5] we can calculate whether the inductors will be able to handle the required current that will be supplied by the powersource. 30 Watt will be supplied to the antenna, represented by P in in equation [5]. The antenna's impedance will be 300 Ω according to simulations, giving a I(rms)equal to 0.45 A.

When the datasheet of the 1008HT inductors is consulted we see that the 1008HT-R56T inductor which we are currently using in our design can handle an rms current of 0.24 A. The inductors have a minimum resistance equal to 5 Ω at 20 MHz, giving a total equal to 30 Ω for the six series inductors.

Where the parallel resistor is the lowest (200 Ω) the current will have a magnitude of 0.39 A. The current through the inductors will be at a maximum where the parallel resistor is equal to 680 Ω, with a magnitude of 0.43 A. The current's magnitude will decrease from the feed towards the end of the antenna.

The current inductor would be able to handle the required power needed for a short period of time, but a parallel configuration of inductors can be used to supply the necessary inductance and would be able to reduce the current through the inductor, thus increasing their operational duration.

Chapter 5

Conclusion

In this project's initial phase several antenna topologies were investigated. For each topology, the component values and positions were optimised numerically to find the design best suited for a low frequency, wideband jamming antenna.

The simulations of the different topologies in FEKO revealed some design criteria. The addition of inductor and resistor loads (RL loads) on an antenna increases the antenna's ability to radiate energy at different frequencies. When a large number of RL loads are spaced from one another, to avoid inductor coupling, the antenna's gain will have an improvement at low frequency and deteriorate at high frequency.

The top-loaded antenna exhibits a high efficiency because the horizontal side arms allow the antenna to have a current distribution larger than zero at the top of the antenna. The results from the antenna with a helix structure, folded structure and top-loaded antenna confirmed that the antennas performance cannot be improved by extending its length while complying with the height specification. The proximity of the added wire to the existing wire also affects the antennas performance at different frequencies because of coupling (inducing of currents and capacitance) between the wires. The cases of the antenna with a helix and folded structure illustrate the coupling between wires located in close proximity of each other.

The use of a RL load was studied using small inductive loads in the form of beads which increased to inductive loads on the boundary of the required operating frequencies (RL chip loads). The RL load's position, magnitude and quantity was investigated on a monopole antenna and compared to the design in which the antenna's length was increased.

The best design topology was found to be that of a normal monopole antenna, with four RL sections added along the length. Each RL section consisted of six inexpensive, commercially available inductors in series and one parallel resistor over the inductors.

Using FEKO to obtain the RL values, the realisation of the antenna was handled in two steps. First a suitable inductor was sourced and the design was checked by importing the measured inductor parameters into FEKO to ensure that the specifications would still be met, using a practical ferrite inductor. The second step was to build and measure the reflection coefficient to test compliance with the VSWR specification. Both the simulated and measured antenna data meet the VSWR specification over the complete bandwidth.

No gain measurement facility for the required frequency range was available to test the experimental antenna's gain against the specifications, due to the low operating frequency. It was thus decided to do near-field probe tests and compare them to the FEKO simulated near-field results. The antennas far-field characteristics would agree with those of the simulation if the measured near-field agrees. These comparisons showed satisfactory agreement in magnitude and phase for the measurements at different heights at a constant distance from the antenna.

Therefore it could be accepted that the antenna will have a gain and SWR equal to that of the simulation. The antenna will have a 10 dB increase in its gain while having a slightly lower SWR. The components used are capable of enduring the required power handling and can be implemented in a parallel configuration for longer working periods.

Future work will include the use of components better suited for the required power handling. Further research on the influence that a human body and an urban environment would have on the practical antenna must still be performed.

Bibliography

[1] Zhang F. F., Sun B. H., Li X. H, Wang W. and Xue J. Y., Design and investigation of broadband monopole antenna loaded with non-foster circuit. *Progress In Electromagnetic Research* C, Vol. 17: 254 – 255, 2010

[2] Hansen, Robert C, "Optimum Loading of Short Whip Antennas", *IEEE Transactions on Vehicular Technology*, Vol VT-24, No. 2 May 1975.

[3] Stewart, W.D. "*Notes on Modelling Short Inductively Loaded Antennas*", Lumped Load Models v. Distributed coils, 2004

[4] Harrison, C. W. "Monopole with inductive loading", *IEEE Transactions on Antennas and Propagation*."Vol 11: 394 – 400, July 1963

[5] Yestrebsky, T. *"Application notes 23, MICRF001 antenna design tutorial"*, The infinite bandwidth company, July 1999

[6] Trusk, Chris "*Magnetic Materials*", Classic works in RF Engineering, Artech House Inc, 3 – 6, 2006

[7] Deasy, Richard E and Cedar Rapids, *Frequency range enhanced monopole antenna*, Nov 1991

[8] Technical Reference Manual for OMNI-A0124-01

[9] Chip Inductor – 1008HT Series (2520) Datasheet, Coilcraft Inc, 2011

[10] Devoldere, John, ON4UN's Low Band DXing, American Radio Relay League,1987

[11] Brown, Bruce F., "Optimum Design of Short Coil-loaded High-Frequency Mobile Antennas", *The ARRL Antenna Compendium*, Vol. 1, ARRL, Newington, CT., 1985

Appendix A: Photographs of measurements and Schematics

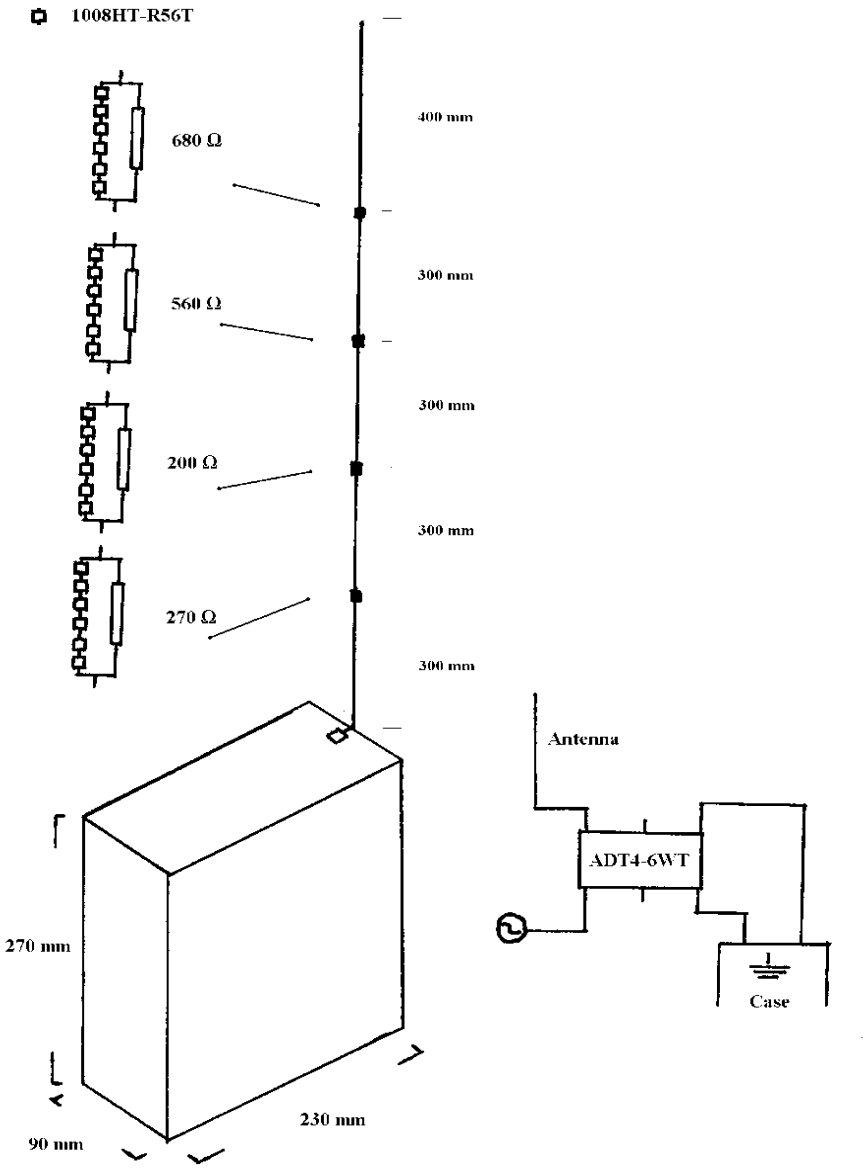

Figure A.1: Antenna layout

Figure A.2: 1008HT-R56T inductive and resistive loaded monopole antenna

Figure A.3: Rohde & Schwarz FSH6 Network Analyser

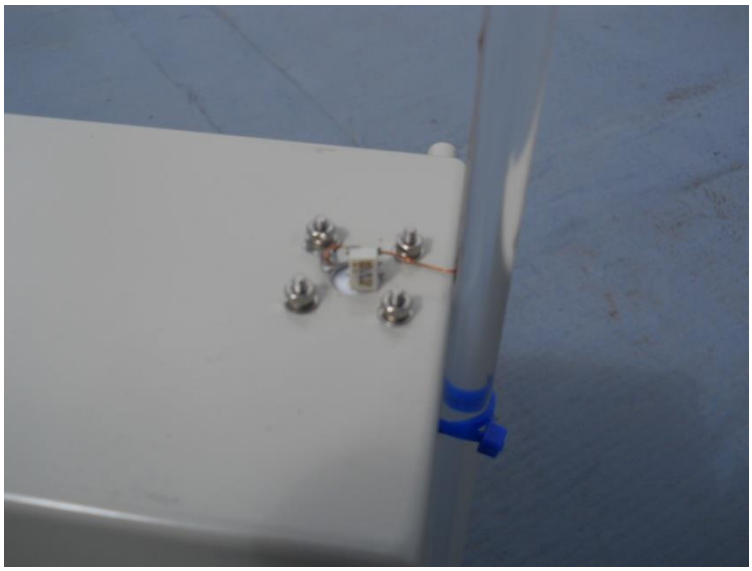

Figure A.4: ADT4-6WT transformer mounted on case

Appendix B: Results of SWR measurements

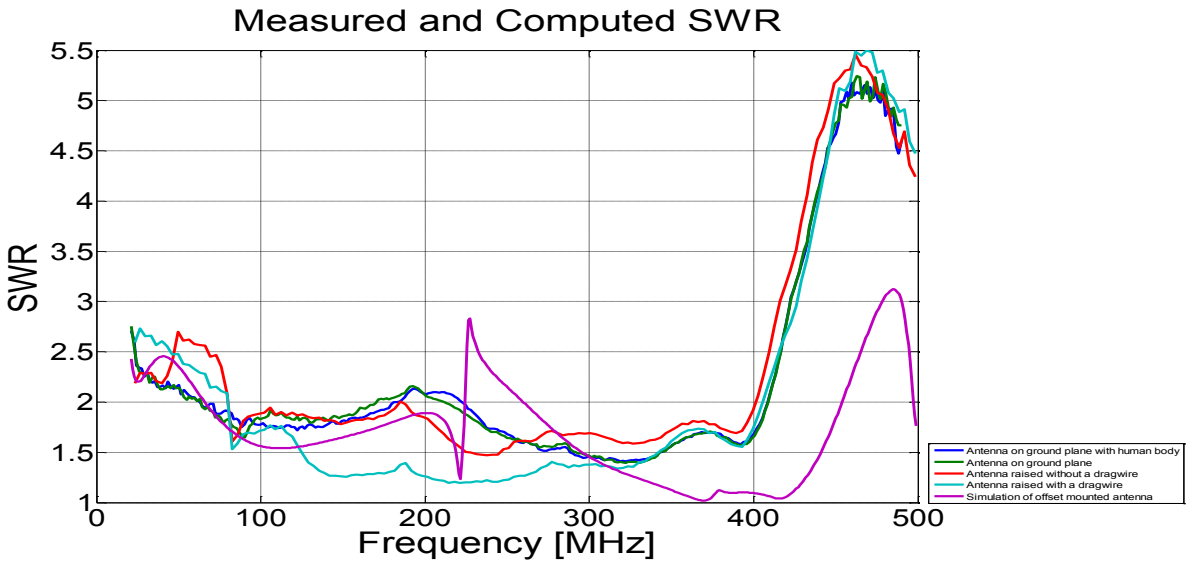

Figure B.1: Standing wave ratio from measured and simulated data with phase shift and 300 Ω reference impedance, antenna on a ground plane with (blue) and without (green) human body in close proximity, raised from ground plane with (cyan) and without (red) drag wire and simulation of corner mounted antenna (magenta)

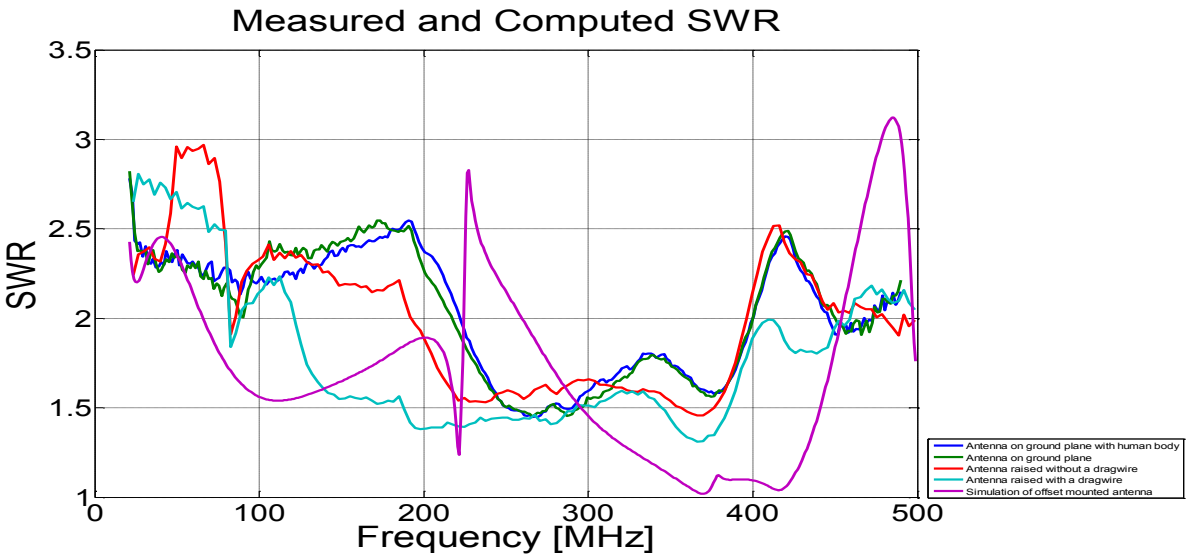

Figure B.2: Standing wave ratio of measurements, with a 300Ω reference impedance and phase compensation, antenna on a ground plane with (blue) and without (green) human body in close proximity, raised from ground plane with (cyan) and without (red) drag wire and simulation of corner mounted antenna (magenta)

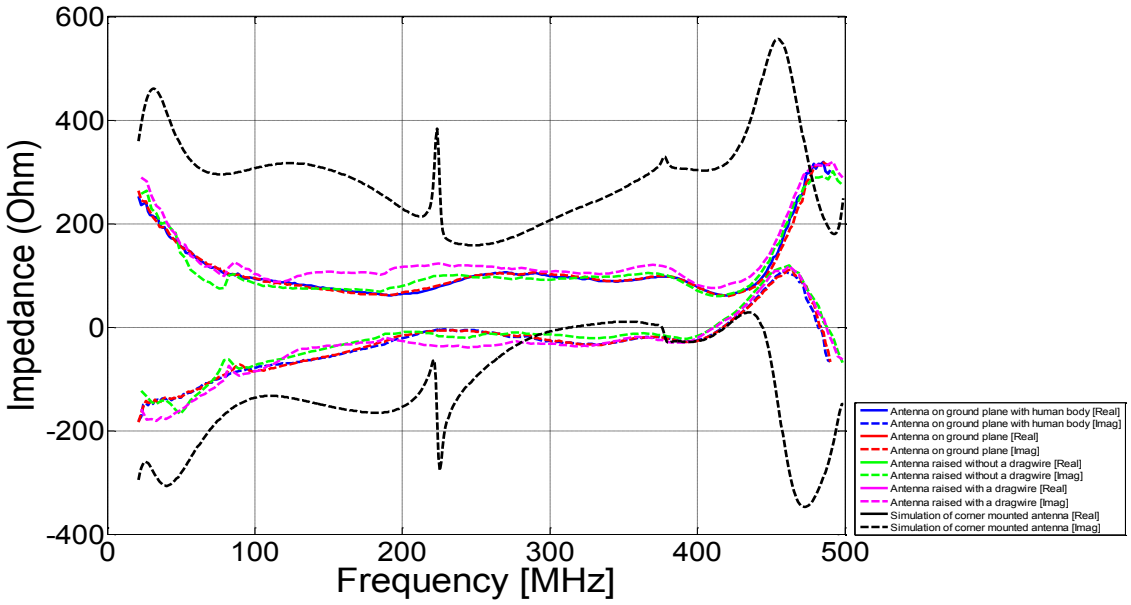

Figure B.3: Impedance of measurements, antenna on a ground plane with (blue) and without (red) human body, raised from ground plane with (magenta) and without (green) drag wire and simulation of corner mounted antenna (black)